

## Wet granular materials

Namiko Mitarai<sup>†\*</sup> and Franco Nori<sup>‡,††</sup>

<sup>†</sup> Department of Physics, Kyushu University 33, Fukuoka 812-8581, Japan.

<sup>‡</sup> Frontier Research System, The Institute of Physical and Chemical Research (RIKEN), Hirosawa 2-1, Wako-shi, Saitama 351-0198, Japan.

<sup>††</sup> Center for Theoretical Physics, Physics Department, Center for the Study of Complex Systems, The University of Michigan, Ann Arbor, Michigan 48109-1040, USA

(Received 00 Month 200x; In final form 00 Month 200x)

Most studies on granular physics have focused on dry granular media, with no liquids between the grains. However, in geology and many real world applications (e.g., food processing, pharmaceuticals, ceramics, civil engineering, constructions, and many industrial applications), liquid is present between the grains. This produces inter-grain cohesion and drastically modifies the mechanical properties of the granular media (e.g., the surface angle can be larger than 90 degrees). Here we present a review of the mechanical properties of wet granular media, with particular emphasis on the effect of cohesion. We also list several open problems that might motivate future studies in this exciting but mostly unexplored field.

*Keywords:* Granular material; Wet grains; Cohesion

### 1 Introduction

#### 1.1 Granular physics and wet granular media

Granular materials are collections of macroscopic particles, like glass beads or sand, which are visible by the naked eye. Because of the macroscopic size of the particles, thermal noise plays no role in particle motion, and particle-particle interactions are dissipative. Therefore, continuous energy input by external forces (gravity, vibrations, etc.) are necessary in order to keep them in motion. Particles may stay at rest like a solid, flow like a liquid, or behave like a gas, depending on the rate of energy input. However, the external force is often not enough for the particles to explore their phase space, which makes them quite different from conventional molecular systems.

The scientific study of granular media has a long history, mainly in the engineering field, and many physicists have joined the granular research com-

---

\*Email: namiko@stat.phys.kyushu-u.ac.jp

munity over the past few decades (for reviews and books, see, e.g., [1–12]). Most studies on granular media, especially in the physics field, have focused on *dry granular materials*, where the effects of interstitial fluids are negligible for the particle dynamics. For dry granular media, the dominant interactions are inelastic collisions and friction, which are short-range and *non-cohesive*. Even in this idealised situation, dry granular media show unique and striking behaviours, which have attracted the attention of many scientists for centuries.

In the real world, however, we often see *wet granular materials*, such as beach sand. Dry and wet granular materials have many aspects in common, but there is one big difference: Wet granular materials are *cohesive* due to surface tension.

In the past, many research groups that studied granular physics have been struggling to minimise humidity and avoid inter-granular cohesive forces (e.g., [13]). Indeed, some experiments were performed in vacuum chambers. Humidity and fluids in general were seen as a nuisance to be avoided at all costs. However, many important real life applications involve mechanical properties of wet granular media. Examples include rain-induced landslides, pharmaceuticals, food processing, mining and construction industries. Thus, it is important to study the mechanical response of granular matter with various degrees of wetness or liquid content.

In this review, we show how the cohesion induced by the liquid changes the mechanical properties of granular materials. We mainly consider static or quasistatic situations, where the cohesion dominates over other effects of the liquid, such as lubrication and viscosity. Some phenomena in this field which are not well-understood are presented below as “open problems”. Most references listed at the end focus on experimental results. Theoretical approaches can be found in the reviews cited below and references therein.

## 1.2 What is different from dry granular media

Studies of wet granular media have been made in many industrial applications. The mechanical properties of wet granular media are also extremely important in geology and civil engineering. For example, let us consider the huge and expensive civil works project of the construction of the Kansai international airport, on a man-made island near Osaka. Because of the weight of the 180 million cubic meters of landfill and facilities, the seabed composed of clay is compressed, and it is inevitable for the airport to sink by some amount; The airport had sunk by 11.7 meters on average at the end of 2000, and the settlement is still carefully monitored [14]. This and other examples from geology and civil engineering stress the need to better understand the mechanical properties of wet granular assemblies, both small and large.

The biggest effect that the liquid in granular media induces is the cohesion

Table 1. Comparison of physical properties between dry and wet granular matter.

| PROPERTY                                | DRY                                  | WET  |
|---|--------------------------------------|--|
| Cohesion                                | Negligible                           | Important  |
| Surface angle                           | Finite<br>Around $35^\circ$ for sand | Finite: Larger than the dry case<br>Can be as large as $90^\circ$ , or even larger |
| Tensile strength                        | Negligible                           | Finite   |
| Yield shear stress                      | Finite<br>Zero at zero normal stress | Finite: Can be larger than the dry case<br>Non-zero at zero normal stress          |
| Hysteresis                              | Yes                                  | Yes: Enhanced  |
| Configurational phase space for packing | Finite                               | Finite: Can be larger than the dry case  |

between grains. Even humidity in the air may result in a tiny liquid bridge at a contact point, which introduces cohesion. The cohesion occurs in wet granular material unless the system becomes over-wet, i.e., the granular medium is completely immersed in a liquid. In this short review, we focus on the effect of this cohesion; the system that we are considering is partially wet granular material, which is a mixture of solid grains, liquid, and air.

In addition to cohesion, there are many effects induced by the presence of the liquid. One of them is the lubrication of solid-solid friction [15–17]. In addition, the liquid viscosity may induce a velocity-dependent behaviour and additional dissipation. These effects are often seen in underwater experiments (e.g., [18,19]). The time scale of liquid motion (how the liquid moves or flows through granular media) also affects the dynamics. All of these effects, of course, play important roles in the properties of wet granular media. However, these are more or less velocity-dependent phenomena, and in the static or quasistatic regime, the cohesion often plays the most important role, providing a significant qualitative difference from dry granular media.

The simplest situation where we see the effect of cohesion in wet granular media would be the sandpiles that children make in a sandbox. Let us first consider a sandpile made of dry grains and afterwards wet grains.

When we make a sandpile using dry sand (Fig. 1(a)), the surface of the pile is smooth, and makes a finite, well-defined angle, which is about  $35^\circ$ . A slightly denser pile might be made by tapping the surface of the pile, but it does not change much the shape of the pile. Even if we try to make a sharper

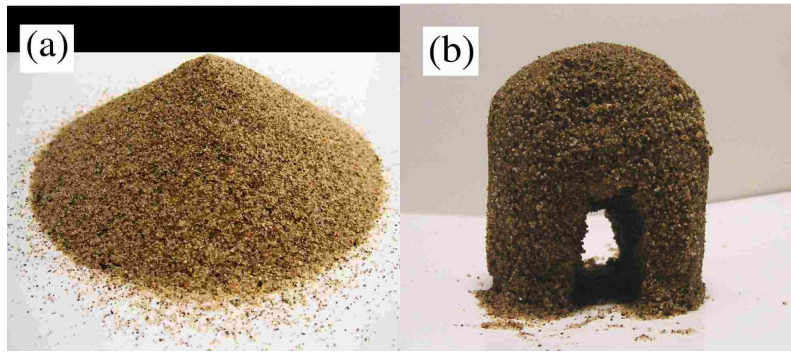


Figure 1. (a) Dry sandpile with a well-defined surface angle. (b) Wet sandpile with a tunnel.



Figure 2. Sandcastle made of wet sand (Copyright Sandscapes 2005).

pile by pouring more dry sand, grains flow down along the pile surface and the resulting angle is always around the same value. It is easy to remove part of the sand from the pile, but we cannot make a tunnel through dry sandpile because the wall around the hole would collapse and the angle of the surface cannot be larger than the critical angle.

Let us add some water to the sand, and make another sandpile (Fig. 1(b)). We can try to find the optimal amount of water to produce a certain shape. Small amounts of water do not allow the creation of many shapes, while too much water results in muddy water that cannot keep a shape. With the proper amount of water, we can make a sandpile with the surface angle larger than the dry case; Indeed, the angle can be as large as  $90^\circ$ , or even larger, allowing the construction of elaborate and stunning sandcastles (see, e.g., Fig. 2). This wet pile can be made denser and stronger by tapping the surface. Now we can make a tunnel through the pile, if we are sufficiently careful. If we try to make a hole that is too large, the pile would break down forming some rugged surfaces.

Therefore, in a sandbox, we already learnt important properties of dry granular media: a finite angle of repose, small hysteresis in packing, and small strength against loading. We also learnt how drastically these properties are changed or enhanced by adding a liquid, resulting in: a much larger angle of repose, stronger hysteresis in packing, and enhanced strength against loading. These comparisons are summarised in Table 1. In the following sections, we will see how these behaviours are studied by scientists.

## 2 Wet granular media: Grains with liquid and air

### 2.1 Cohesion between two spheres

**2.1.1 Meniscus and suction.** Cohesion in wet granular media arises from surface tension and capillary effects of the liquid. Consider a meniscus between air with pressure  $P_a$  and liquid with pressure  $P_l$ . The pressure difference  $\Delta P$  between liquid and air with a meniscus of curvature radii  $r_1$  and  $r_2$  is given by the Young-Laplace equation as

$$\Delta P = P_a - P_l = \gamma \left[ \frac{1}{r_1} + \frac{1}{r_2} \right], \quad (1)$$

where  $\gamma$  is the surface tension between air and the liquid, and the curvature is positive when the meniscus is drawn back into the liquid phase (e.g., [20]). When the curvature is positive,  $\Delta P$  is positive, and it is often called the suction.

The capillary length

$$a = \sqrt{\frac{2\gamma}{\rho_l g}} \quad (2)$$

gives the length scale that compares the capillary force and gravity, where  $g$

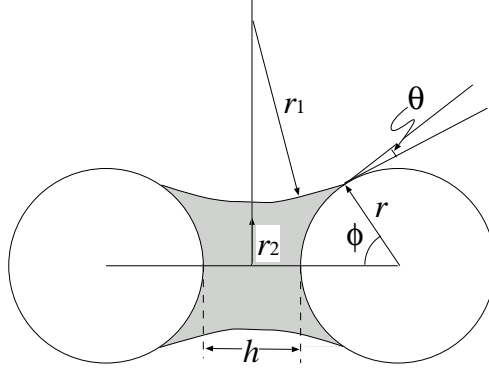


Figure 3. Schematic diagram of a liquid bridge between identical spheres.

is the gravitational acceleration and  $\rho_l$  is the mass density of the liquid;  $a$  is around 3.9 mm for water at room temperature. The capillary force becomes dominant when the relevant length scales are much smaller than  $a$ . Hereafter we consider the situation where the capillary force is dominant. In general, one needs to consider the capillary length when interpreting experimental results, because most experiments are conducted under gravity.

**2.1.2 Liquid bridge between two spheres.** Now let us see how the liquid induces cohesion in granular media by considering a liquid bridge between two identical spheres as shown in Fig. 3. The attracting force between spheres due to the liquid menisci is given by the sum of the surface tension and the suction; when we estimate the force at the neck of the bridge, it is given by

$$F_{\text{bridge}} = 2\pi r_2 \gamma + \pi r_2^2 \Delta P, \quad (3)$$

with

$$\Delta P = \gamma \left[ \frac{1}{r_1} - \frac{1}{r_2} \right]. \quad (4)$$

The detailed experimental analysis of the cohesion force due to the liquid bridge between two spheres is found in [21]. The effect of roughness on the cohesive force is discussed in detail in [22].

In real partially wet granular media, the picture of a liquid bridge formed between completely spherical particles is often not sufficient to describe the interaction. However, the presence of a liquid, which tries to minimise its surface area, generally results in suction and a cohesive force between particles.

## 2.2 Wet granular media with various liquid content

**2.2.1 Four states of liquid content: pendular, funicular, capillary, and slurry state.** It is well known that cohesion in wet granular materials depends on the amount of liquid in the system. The following four regimes of liquid content have been distinguished in wet granular media [23, 24]:

- Pendular state: Particles are held together by liquid bridges at their contact points.
- Funicular state: Some pores are fully saturated by liquid, but there still remain voids filled with air.
- Capillary state: All voids between particles are filled with liquid, but the surface liquid is drawn back into the pores under capillary action.
- Slurry state: Particles are fully immersed in liquid and the surface of liquid is convex, i.e., no capillary action at the surface.

These four regimes are schematically shown in Table 2.

Cohesion arises in the pendular, funicular, and capillary states. Thus, we consider these three states in this review. A priori, the mechanical properties of these three states would be expected to be qualitatively different. In the case of the pendular state, the cohesive force between a pair of grains acts through a liquid bridge; while in the capillary state the interface between the liquid and the air is pressed due to the suction and that pressure keeps together all the grains in the liquid phase. Both the two-body cohesion due to liquid bridges and the suction at the liquid-air interfaces play important roles in the funicular state.

It is very difficult to directly observe the liquid distribution in three-dimensional granular assemblies, though the liquid distribution should be readily observable for two-dimensional wet granular aggregates confined by Plexiglas plates (cf. [25]). As we will see later, liquid bridges in three dimensions for rather small liquid content have recently been visualised by using index matching techniques [22, 26, 27], but it seems to be difficult to extend the method for much larger liquid content. The detailed liquid distribution in the each liquid content regimes described in Table 2 still remains as one of many “open problems” that we list below as areas that have not been sufficiently well studied so far.

Conventionally, these liquid content regimes have been distinguished by measuring the relation between the liquid content  $S$  and the suction  $\Delta P$  [23] as we will see below, where  $S$  is the ratio of the volume of liquid  $V_l$  in the system to the volume of the voids  $V_v$  in the granular media (when the total volume of the system is  $V_t$  and the volume occupied by grains is  $V_s$ , then  $V_v = V_t - V_s$  and  $V_v = V_l + V_a$  where  $V_a$  is the air volume in the system). Some authors define  $S$  as the percentage of the liquid content (i.e., multiplying the ratio of

Table 2. Granular media with various amounts of liquid [23, 24]. In the schematic diagrams in the third column, the filled circles represent the grains and the grey regions represent the interstitial liquid.

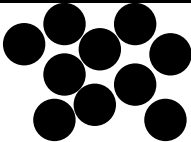
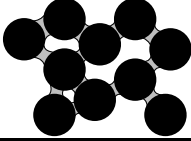
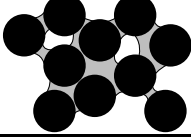
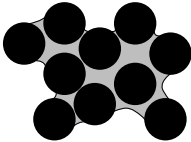
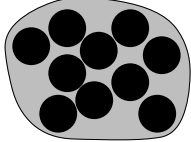
| Liquid content   | State     | Schematic diagram   | Physical description  |
|------------------|-----------|---|---|
| No               | Dry       |    | Cohesion between grains is negligible.  |
| Small            | Pendular  |    | Liquid bridges are formed at the contact points of grains. Cohesive forces act through the liquid bridges.  |
| Middle           | Funicular |    | Liquid bridges around the contact points and liquid-filled pores coexist. Both give rise to cohesion between particles.   |
| Almost saturated | Capillary |   | Almost all the pores are filled with the liquid, but the liquid surface forms menisci and the liquid pressure is lower than the air pressure. This suction results in a cohesive interaction between particles. |
| More             | Slurry    |  | The liquid pressure is equal to, or higher than, the air pressure. No cohesive interaction appears between particles.   |



Table 3. List of methods to measure the suction and practical suction range for each measurement. Methods based on the osmotic pressure difference (e.g., due to gradients of solute concentration) are not listed below. Adapted from [28].

| Technique or Sensor                        | Suction Range (kPa) | References |
|--|---------------------|------------|
| Tensiometers                               | 0-100               | [29, 30]   |
| Axis translation techniques                | 0-1500              | [31, 32]   |
| Electrical or thermal conductivity sensors | 0-400               | [33–35]    |
| Contact filter paper method                | Entire range        | [36]       |

$S = V_l/V_v$  by 100). Here, either case, ratio or percentage, is clear from the text.

### 2.2.2 Liquid content and suction.

**Measurement of suction in granular media.** There are several ways to measure the suction  $\Delta P$  in granular media, and the appropriate method should be chosen regarding the measurement range of  $\Delta P$ . Table 3 shows the list of methods and the range of measurements [28] commonly used in soil mechanics (where the mixture of soil grains and water is considered as a specimen).<sup>1</sup> It is beyond the scope of this brief review to describe all the experimental methods used, but these are described in the references. As examples, below we describe two often-used methods, called the axis-translation techniques and tensiometers, which make use of the capillary pressure in a porous ceramic disk to measure and to control the suction [28].

Relatively low suction can be measured or controlled by using tensiometers and the axis-translation technique [28]. A schematic diagram to describe these methods is given in Fig. 4; These methods make use of the properties of what is called a “high-air-entry (HAE) material”, which is a material with many microscopic pores, such as a porous ceramic. In Fig. 4, a container is separated in two parts by a HAE disk; the bottom part of the box is filled with a liquid with pressure  $P_l$ , while the upper part is filled with air with pressure  $P_a$ . A magnified view of the HAE disk is given in the inset (a), where the pores

---

<sup>1</sup>When solutes are dissolved in water in soil, the osmotic effects produce the chemical potential difference from free water, where free water is the water that contains no dissolved solute, has no interactions with other phases that produce curvature to the air-water interface, and has no external force other than gravity [28]. In the soil mechanics, this chemical potential difference is sometimes measured in the unit of pressure, and it is referred to as osmotic suction. The pressure difference between the air and liquid (water) in soil  $\Delta P = P_a - P_l$ , which is due to capillary effect and short-range adsorption of water to grain surfaces, is referred to as matric suction. In this paper, we focus on the latter, and  $\Delta P$  is simply referred to as suction.

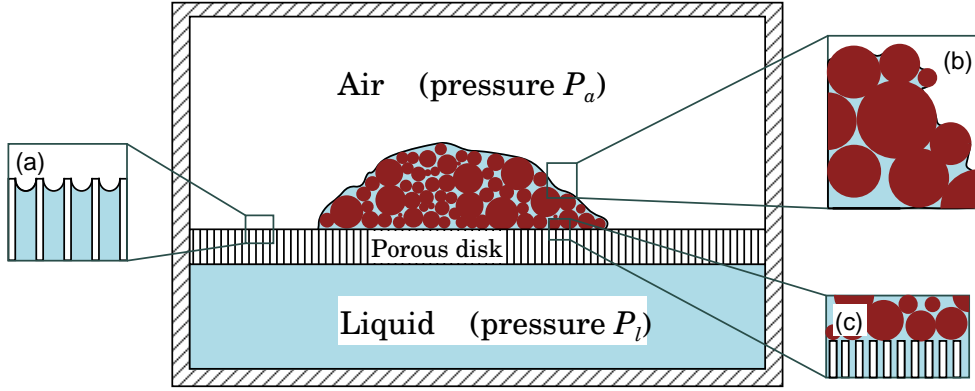


Figure 4. Schematic diagram describing the tensiometers and the axis-translation techniques. The filled circles represent grains and the light blue region represents a liquid. The container is separated by a High-Air-Entry (HAE) porous disk that has many microscopic pores. The upper part is filled with air with pressure  $P_a$ , and the lower part is filled with liquid with pressure  $P_l$ . The pores in the porous disk are filled with liquid, and the menisci at the top surface of the pores in the porous disk (a magnified view is shown in inset (a)) make it possible to keep  $P_l < P_a$ . A wet granular assembly is placed on the porous disk (a magnified view is shown in inset (b)), and liquid in the wet granular media is in good contact with the liquid in the porous disk (a magnified view is shown in inset (c)); the liquid pressure around the wet grains equals the pressure  $P_l$  of the bulk liquid in the bottom of the container. Adapted from [28].

of the HAE material are saturated with liquid. There, the surface tension at the liquid-air interfaces formed in the pores allow a finite pressure difference between the liquid and air. Considering Eq. (1) and the magnified view (a) in Fig. 4, the largest possible pressure difference between the air and liquid in the HAE material is roughly given by

$$\Delta P_{\max} = \frac{2\gamma}{R_{\max}}. \quad (5)$$

Here, as a first approximation, we assume that the pores are tube-shaped with maximum radius  $R_{\max}$ ; for smaller pore size,  $\Delta P_{\max}$  would be larger. The liquid pressure  $P_l$  in the lower part of the container and the air pressure  $P_a$  in the upper part can be separately controlled without allowing the air to enter the lower part of the container, as far as  $(P_a - P_l) < \Delta P_{\max}$  is satisfied.

Now, let us place a wet granular material on the HAE disk inside the container (Fig. 4, inset (b)) [28]. When the equilibrium is reached after a long enough waiting time, the liquid pressure in the wet granular medium should be equal to the liquid pressure  $P_l$  in the lower part of the container, if the liquid phase in the granular medium is in good contact with the liquid in the pores of the HAE disk (Fig. 4, inset (c)). The air pressure  $P_a$  and the liquid pressure  $P_l$  in the upper and lower parts of the container, respectively, can be easily measured, or even controlled, and the suction  $\Delta P$  in the wet granular

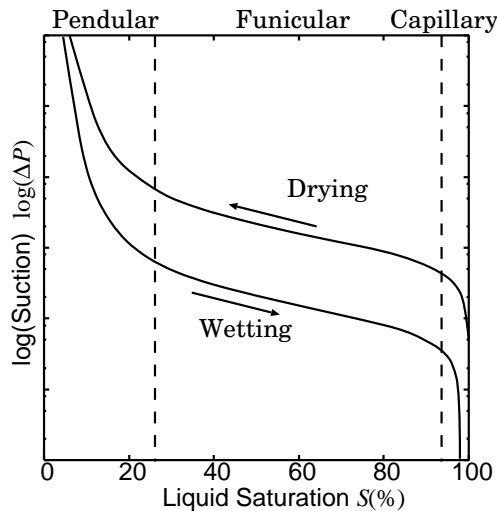


Figure 5. A schematic plot of the suction  $\Delta P$  versus the liquid content  $S$ . The suction is shown in a log-scale. The upper curve represents the drying process, and the lower curve represents the wetting process. It changes the slope significantly near the phase boundaries between the pendular, funicular, and capillary states.

material is given by  $\Delta P = P_a - P_l$  [28].

The method to control the suction  $\Delta P$  by controlling the liquid and air pressures separately is called the axis-translation technique [28]. Initially a saturated granular material is placed on a HAE disk that separates the liquid and the air, as schematically shown in Fig. 4, and the liquid in the granular assembly is drained until the system reaches the equilibrium, where the liquid pressure in the granular medium becomes equal to that of the bulk liquid in the lower box. The tool to measure the suction by using the HAE disk is called a tensiometer, which is composed of a cup made of a HAE ceramic and a sensor to measure the liquid pressure, connected by a tube filled with liquid (water) [28]. The HAE ceramic cup is placed in the wet granular assembly, and the pore pressure is measured by a direct exchange of liquid between the sensor and the wet granular medium. Note that, in using either the axis-translation technique or a tensiometer, the maximum possible value of the suction is limited by  $\Delta P_{\max}$ ; other methods used to measure larger pressure differences are listed in Table 3 and Ref. [28].

**Relation between the liquid content and suction.** The schematic description of the suction  $\Delta P$  versus the liquid content  $S$  is shown in Fig. 5 [23, 28]. Two lines are shown because there is a hysteresis in the wetting and drying processes. In both lines, the slope for low and large liquid content is much larger than that for intermediate liquid content. This change of slope reflects

the liquid distribution in granular media.

For simplicity, let us consider the drying process (the drainage of liquid) from completely saturated granular media. At first the material is in the slurry state, and the liquid pressure is the same or larger than the air pressure. After an appropriate amount of liquid is drained, the media is in the capillary state, and the liquid pressure becomes lower than the air pressure, i.e., the suction  $\Delta P$  becomes positive. When we further decrease the liquid content  $S$  in the capillary state,  $\Delta P$  increases very rapidly upon decreasing  $S$ ;  $\Delta P$  is determined by the curvature of the liquid surface, and the change of the surface curvature requires little change of liquid content  $S$  because bulk liquid remains in the system. When  $\Delta P$  exceeds a critical value, which is mainly determined by the surface tension and the geometry of granular media around the surface liquid, air starts to enter the bulk of the system and the funicular state is obtained. The suction still increases as the liquid content decreases, but its rate of increase becomes much smaller than that in the capillary state, because the liquid in the pores in the bulk needs to be removed. At some point, most of the voids will be filled with air, and the rest of the liquid is found around the contact points between neighbouring grains and in the thin liquid film that covers the grains' surfaces. Namely, the system is in the pendular state. In this pendular state, a small change of the liquid content again results in a relatively large change of the suction, because the total amount of the liquid is much smaller than the void volume  $V_v$  and the change of curvature at each liquid bridge requires only a small change of the liquid content  $S$ .

As shown in Fig. 5, for a given value of the suction  $\Delta P$ , the liquid content  $S$  is smaller for the wetting process of initially dry granular media than that of the drying process of initially saturated grains. This is partly because of the hysteresis in the wetting and drying processes at solid surfaces [22, 37, 38], and partly because the variation of the pore size in the granular medium [28]. The flow of liquid in porous media (including granular media) is an important and interesting problem; indeed, this problem has developed into a separate research area. For a recent review on this problem, in terms of statistical physics, see [39].

### 3 Mechanical properties

In this section, we summarise what is known about the mechanical properties of wet granular media. As mentioned above, here we focus on granular cohesion in the static and quasistatic regimes for varying liquid content. To also have some idea about the dynamics, dynamical experiments are briefly presented in the final part of this section.

### 3.1 Granular cohesion in the static and quasistatic regimes

**3.1.1 Compaction of wet granular media.** The configuration of grains in a container shows history-dependence. In the case of dry granular media, the material just poured in a container is compacted when it is tapped. The dynamics of this compaction process is slow, which is known to show logarithmic dependence on the number of taps (e.g., [40–42]).

In the case of wet granular media, very low-density configurations can be realised even when the grains are spherical. Due to the cohesion, a configuration with many large openings or gaps surrounded by chains of particles can be stabilised, which may not be stable for dry spherical grains [43]. The compaction via a ram of this low-density configuration by a quasistatic compression has been examined [44, 45]. With increasing pressure on the system, the relatively large openings between particles disappear; a grain in a chain snaps in away from the chain, and the chain structure changes. After the openings disappear, a high-density region is formed, and the density difference between the initial low-density and newly-formed high-density regions becomes clearly visible. One can see that the domain wall between the high-density and low-density regions travels through the system like a wave.

The realisability of very low-density structures indicates that the hysteresis of configurations in wet granular media can be stronger than that in dry granular media. In other words, the many huge gaps or openings that are possible in wet granular media, make the configuration phase space available to the grains much larger than the dry granular case (see also Table 1).

#### 3.1.2 Angle of repose for small amounts of liquid.

**Experiments.** The angle of repose  $\theta_r$  and the critical angle  $\theta_c$  are measurable quantities that are sensitive to the cohesion. Here, the critical angle  $\theta_c$  is the surface angle just before an avalanche occurs, while the angle of repose  $\theta_r$  is the surface angle after the avalanche, and is typically slightly smaller than  $\theta_c$ . When the amount of liquid is small, the cohesion is also small, but the cohesion is still detectable through  $\theta_r$  and  $\theta_c$  of either a granular pile or in a drum that rotates very slowly [46–51].

Even the humidity in the air is enough to induce cohesion for initially dry granular material [46, 49, 52–57]. Bocquet *et al.* [46] measured the critical angle  $\theta_c$  of glass beads in humid air, and found that  $\theta_c$  depends on the waiting time  $t_w$ , namely, how long they waited after preparing the sample until measurement. They reported the relation  $(\tan \theta_c - \tan \theta_0) \propto \log(t_w) / \cos \theta_c$ , where  $\theta_0$  is a constant (Fig. 6), and also found that the  $t_w$ -dependence of  $\theta_c$  varies with humidity.

This time dependence of the critical angle  $\theta_c$  on the waiting time  $t_w$  has been

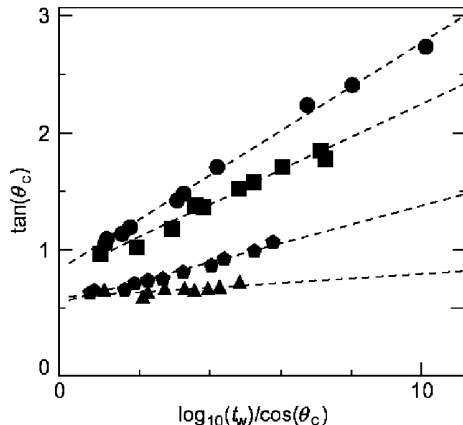


Figure 6. The critical angle  $\theta_c$  of glass beads in humid air as a function of the waiting time  $t_w$  in a slowly rotating drum, shown as  $\tan \theta_c$  versus  $(\log_{10} t_w / \cos \theta_c)$ . The time is in units of seconds, and humidities are 15% (triangles), 27% (pentagons), 36.1% (squares), and 45.5% (circles). As time passes, more and more liquid condenses at the contact points between particles, increasing the cohesion between them. Therefore, the critical angle increases with time. From [46].

analysed based on the capillary condensation, which results from the fact that the equilibrium vapour pressure in a narrow space where non-zero suction  $\Delta P$  is allowed is lower than that in the bulk [58].<sup>1</sup> Due to this effect, the vapour can condense for lower pressures in a narrow space, like the point where particles are in contact, resulting in tiny liquid bridges at the contact points between touching grains. The critical angle  $\theta_c$  increases due to the cohesion from these tiny bridges, which becomes larger and increases with time because more and more vapour condenses.<sup>2</sup>

Hornbaker *et al.* [47] investigated the angle of repose  $\theta_r$  of spherical polystyrene beads mixed with either corn oil or vacuum-pump oil by the draining-crater method. They measured the liquid content dependence of the angle of repose  $\theta_r$ . They found that  $\theta_r$  increases linearly with the average oil-layer thickness  $\delta_{\text{liq}}$  (the volume of oil added divided by the total surface area of particles), indicating that the cohesion increases as the amount of liquid

<sup>1</sup>“Capillary condensation” can be understood as follows. Consider air and liquid in a box, where the liquid pressure  $p_l$ , the total air pressure is  $p_a$ , the liquid vapour pressure  $p_v$ , and dry air pressure  $p_{da} = p_a - p_v$ . From the Gibbs-Duhem equilibrium criterion and ideal gas approximation for the air, the Kelvin’s equation [58] is obtained:  $p_v = p_{v0} \exp[-(\Delta P v_l)/(R_g T)]$ , where  $v_l$  is the partial molar volume of liquid,  $p_{v0}$  is the saturated vapour pressure,  $T$  is the absolute temperature, and  $R_g$  is the gas constant. Thus, when  $\Delta P > 0$ ,  $p_v$  becomes smaller than  $p_{v0}$ . Namely, in narrow spaces like pores in granular media, the vapour can condense for lower vapour pressures.

<sup>2</sup>It should be noted, however, that there are alternative explanations about the origin of cohesion in this experiment. Restagno *et al.* [52] conducted similar experiments for glass beads with water and glass beads with ethanol, and found that the difference in the increase of the critical angle is larger than the value expected from the difference of the surface tension between water and ethanol. This might be partly due to the chemical reaction between silica and water [52, 59].

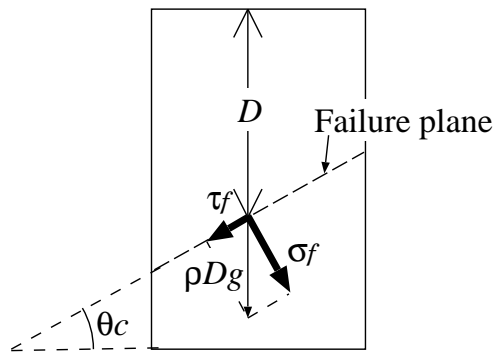


Figure 7. Schematic diagram of the force balance at the failure plane, as determined by the Mohr-Coulomb failure criterion.

increases. However, as they increased the liquid content, particles started to form correlated particle clusters (clumps), and finally  $\theta_r$  could not be determined in a well-defined manner. The distribution width of the measured angle of repose became suddenly wide for a certain amount of liquid, suggesting a transition to a situation where long-range correlations dominate.

**Cohesion and angle of repose.** The observed increase of  $\theta_r$  and  $\theta_c$  with increasing liquid content should be due to the cohesive force between grains. The relation between the surface angle and cohesion, however, has not yet been clearly understood. This is an area that would greatly benefit from more systematic studies.

The most well-known analysis of the critical angle  $\theta_c$  in granular engineering is to use the failure condition for a continuum description [3, 50]. In the case without cohesion, a phenomenological failure criterion for granular media is given in terms of the shear stress  $\tau$  and the normal compressible stress  $\sigma$  as

$$\tau > \mu\sigma, \quad (6)$$

where  $\mu$  is the internal friction coefficient, considered as a material parameter. If there is any plane for which the ratio  $\tau/\sigma$  exceeds  $\mu$ , the material fails at that plane;  $\tau_f/\sigma_f = \mu$ , where the subscript  $f$  for the stresses  $\tau_f$  and  $\sigma_f$  indicates the value at the failure plane. The critical angle corresponds to the angle of this failure plane, where the failure starts. At the same time, because the stress comes from the weight above the plane, as schematically shown in Fig. 7, we have

$$\tau_f = \rho g D \sin \theta_c \quad \text{and} \quad \sigma_f = \rho g D \cos \theta_c, \quad (7)$$

with mass density  $\rho$  and the depth  $D$  of the failure plane from the surface

before failure. Namely, we have

$$\frac{\tau_f}{\sigma_f} = \tan \theta_c = \mu, \quad (8)$$

which gives  $\theta_c$  for dry granular media.

In the case of wet granular media, it has been considered that the cohesion result in a normal cohesive pressure  $\sigma_c$  [3, 50]. This additional normal stress  $\sigma_c$  allows to support a finite shear stress, even in the limit of zero applied normal stress  $\sigma$ . Then, the criterion in Eq. (6), for non-cohesive material, is modified into [3, 50]

$$\tau > \mu(\sigma + \sigma_c). \quad (9)$$

The criterion in Eq. (9) is called the Mohr-Coulomb criterion, and Eq. (6) is the special case of Eq. (9) with  $\sigma_c = 0$ . With non-zero  $\sigma_c$ , the stresses at the failure plane satisfies  $\tau_f = \mu(\sigma_f + \sigma_c)$ , while we still have Eq. (7) for the force balance. Then we have

$$\mu = \tan \theta_c \left( 1 + \frac{\sigma_c}{\rho g D \cos \theta_c} \right)^{-1}, \quad (10)$$

which shows that  $\theta_c$  decreases with increasing  $D$ . Namely, the criterion is the strictest at the bottom of the sandpile, which has the largest  $D$ . Therefore, the failure occurs at the bottom of the sandpile, and Eq. (10) with  $D$  being the total depth of the sandpile gives the critical angle  $\theta_c$  of that sandpile. Note that the relation for the non-cohesive case, Eq. (8), is recovered in the limit of  $D \rightarrow \infty$ ; the frictional force that holds the pile increases with the size of the pile because the normal pressure increases, but the cohesive force remains constant, thus the cohesive force becomes irrelevant in a large enough granular pile [3, 50]. We have increasing critical angle due to cohesion only for a finite sandpile where  $\sigma_c/\rho g D$  is finite, and within this range  $\theta_c$  increases with the cohesive stress  $\sigma_c$  and depends on the pile size. Note that, in this Mohr-Coulomb criterion, the yield shear stress is the consequence of the increased normal pressure, and the direct contribution of particle-particle cohesion to the shear stress is not taken into account.

In the case of the pendular state, the cohesive stress  $\sigma_c$  arises from the liquid bridges between particles. Rumpf [60] proposed a simple model to estimate the cohesive stress from the force per bridge in isotropic granular media of identical spheres with diameter  $d$ , ignoring the effect of distributions in liquid bridge sizes and in number of bridges per particles [27]. He estimated the cohesive



force  $\sigma_c$  per unit area as

$$\sigma_c \approx \nu \frac{k}{\pi d^2} F, \quad (11)$$

where  $\nu$  is the packing fraction of the grains,  $k$  is the average number of liquid bridges per particle, and  $F$  is the average force per liquid bridge.<sup>1</sup>

According to the Rumpf model in Eq. (11),  $\sigma_c$  is proportional to the cohesion per liquid bridge  $F$ . Then, the fact that  $\theta_r$  for wet spherical glass beads increases with liquid content [47] may suggest increasing  $F$  by increasing the liquid bridge volume, if the number of bridge per particle  $k$  stays constant. However, this cannot be understood by simply considering the pendular state for completely spherical beads. For the case when two spheres are in contact ( $h = 0$ ) and the wetting angle  $\theta = 0$ , we get from Eq. (3) that

$$F_{\text{bridge}} = \frac{2\pi r \gamma}{1 + \tan(\phi/2)}, \quad (12)$$

where  $r$  is the radius of the spheres and  $\phi$  is given in Fig. 3. Equation (12) gives  $\partial F_{\text{bridge}}/\partial \phi < 0$ . Namely, the attracting force  $F_{\text{bridge}}$  becomes smaller as the amount of liquid in the bridge increases while keeping the particle separation equal to zero.

This discrepancy can be resolved by considering the surface roughness of the grains [48,50]. It has been known that, in the case of the cone-plane contact, the attracting force increases when the amount of liquid increases [61]. If the liquid bridge volume is small enough to neglect the curvature of the macroscopic spherical shape of the beads, the surface roughness becomes more relevant, and the geometry at the contact point can be considered as the cone-plane type. If the liquid bridge becomes wide enough compared to the macroscopic curvature of the surface, then the estimation for spheres in Eq. (12) is expected to work.

Mason *et al.* [26] experimentally observed how the liquid distributes in spherical beads with microscopic surface roughness. They found that, when the amount of liquid is smaller than a critical value, most of the liquid is trapped on the particle surface due to the surface roughness (Fig.8(a)) and the critical angle did not depend on the surface tension of the liquid. When the liquid content exceeds a critical value, liquid bridges are formed at the contact points (Fig.8(b)), and the critical angle increases with liquid volume and depends on the liquid surface tension. This agrees with the behaviour expected from

---

<sup>1</sup>In papers on granular engineering including [60], the porosity  $n$  defined as the ratio of the void volume  $V_v$  to the total volume  $V_t$  is often used instead of the packing fraction  $\nu$  as a parameter to characterise the packing. These parameters are related by  $n = 1 - \nu$ .

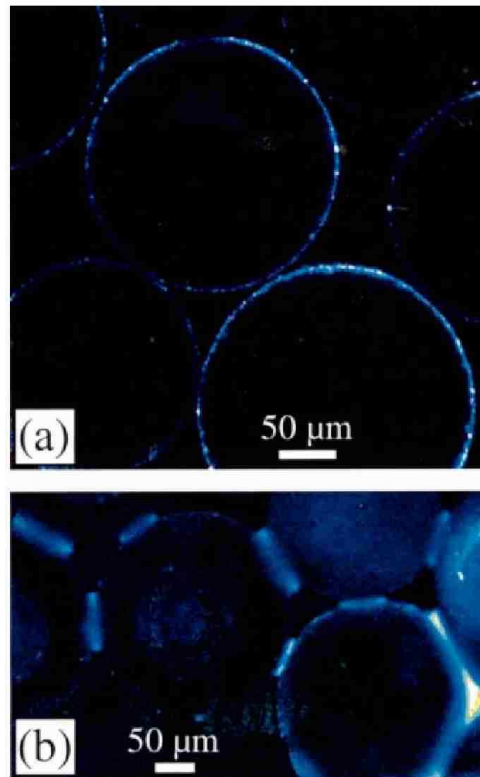


Figure 8. Distribution of small amount of liquid in granular media. The blue region shows the location of the liquid. The average grain diameter is  $240 \mu\text{m}$ . (a) When the amount of liquid is small, the liquid is uniformly distributed at the grain surface. (b) When the amount of liquid is large enough, most of the liquid is caught at the contact points between particles and liquid bridges are formed. From [26].

the regime where the surface roughness determines the cohesion from a liquid bridge.

However, one should note that, not only the cohesion force  $F$  but also the number of liquid bridges  $k$  per particles depends on the liquid content in general, which should also affect the cohesive stress  $\sigma_c$ . Recent experiments [27, 62] show that  $k$  increase very rapidly upon liquid content for small liquid content, and then saturate. The effect of  $k$  on the critical angle needs to be investigated carefully especially for small liquid content.

Albert *et al.* [48] proposed a criterion to understand the critical angle different from the Mohr-Coulomb criterion. They considered the criterion whether a grain at the surface escapes from the bumpy geometry that other grains form. In their theory, the surface grain at an unstable position rolls down and the final angle is determined by the condition that all grains at the surface sit at stable positions. The cohesion from liquid affects the force balance and

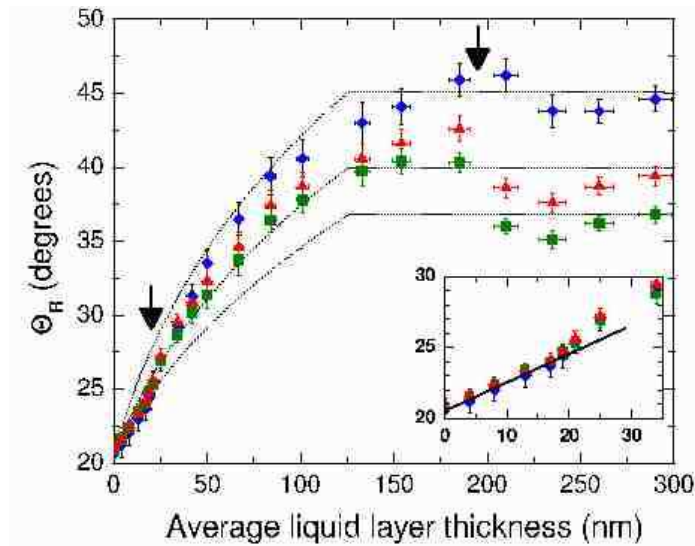


Figure 9. Angle of repose  $\theta_r$  versus the average oil-layer thickness  $\delta_{liq}$  for spherical glass beads with average diameter 0.9mm with three different container diameters  $d_c$  (diamonds: 10.3cm, triangles: 15.6cm, squares: 20.4cm). The inset shows an enlargement of small  $\delta_{liq}$  regime. The two vertical arrows indicate the transitions between the granular, correlated, and plastic regime. From [63].

increases the critical angle  $\theta_c$ .

In either mechanism, the Mohr-Coulomb criterion or the surface failure criterion, the angle of repose of cohesive granular media is larger than that of non-cohesive granular media. However, the location of the failure plane is different. The failure occurs at the bottom in the case of the Mohr-Coulomb criterion and  $\theta_c$  depends on the system size, while the surface fails for the “grain escape” criterion and  $\theta_c$  is independent of the system size. In addition, the Mohr-Coulomb criterion is a continuous description, while the grain escape criterion explicitly considers the discreteness of the system.

Both mechanisms may be responsible in determining the critical angle. However, it is likely that the discrete picture is dominant for very small amounts of liquid content, with small cohesive bulk stress, while the continuous picture is appropriate when the liquid content is enough to cause the cohesive bulk stress comparable to gravity. In order to see the relevant mechanism, Tegzes *et al.* [63] examined the system size dependence of the angle of repose  $\theta_r$  for a larger range of liquid content (Fig. 9). They adopted the draining crater method, and the system size is controlled by changing cylinder diameters. They found that  $\theta_r$  is independent of system size for small enough liquid content (called the *granular regime*, where surface flow occurs at the top few layers), while it decreases with system size for larger liquid content (called the *corre-*

*lated regime*, where grains form clumps and the surface flow is correlated). At the largest liquid content, the angle first decreases and then increases slightly with oil-layer thickness, but still depends on the system size (called the *plastic regime*, where the medium retains a smooth crater surface and the motion is coherent). Qualitative agreements have been obtained with the surface failure criterion for the granular regime and with the Mohr-Coulomb criterion for the correlated and plastic regime.

These results are not yet conclusive, and many researches on the surface angle are still going on. Ertas *et al.* [64] considered the critical angle in a pile made of a mixture of spheres and dumbbell-shape grains, extending the surface failure criterion by [48]. They found that the surface angle drastically increases as the fraction of dumbbell-shape grains increases, because the dumbbell-shape grains hardly roll down the slope. They pointed out that, in wet granular media with small liquid content, liquid bridges connect a few grains and make clumps; these clumps may contribute to the increasing surface angle through the same mechanism that the fraction of dumbbell-shaped grains increased the critical angle. On the other hand, Nowak *et al.* [65] applied the geometrical consideration of force balance by [48] not only at the surface but also inside the material. They claimed that the most unstable plane from the geometrical consideration is inside the material. Their argument does not take into account the effect of friction, but it gives system-size dependent critical angle that agree with the critical angle of dry grains in the limit of infinite system size; this feature is similar to that in the Mohr-Coulomb criterion.

In summary, the effect of cohesion on surface angle in granular pile has not yet been clearly understood, and further systematic studies are needed.

**3.1.3 Tensile, compression, and shear tests for intermediate and large liquid content.** For large enough cohesion, the angle of repose may exceed  $90^\circ$  for laboratory-scale granular piles. In such a regime, the angle of repose is no longer a good parameter to characterise the cohesion, and we need another method to characterise the cohesion in wet granular media.

If the failure condition is characterised by the Mohr-Coulomb criterion (9), the measurement of the stresses at the failure gives the cohesive stress  $\sigma_c$ , which characterises the cohesion in wet granular media. The analysis of granular media based on the Mohr-Coulomb criterion has been well-established in the engineering field, and a considerable amount of data has been accumulated for wet granular media. In this subsection, we briefly describe several experimental methods to determine the internal friction coefficient  $\mu$  and the cohesive stress  $\sigma_c$ , and summarise what has been known for wet granular media from those measurements.

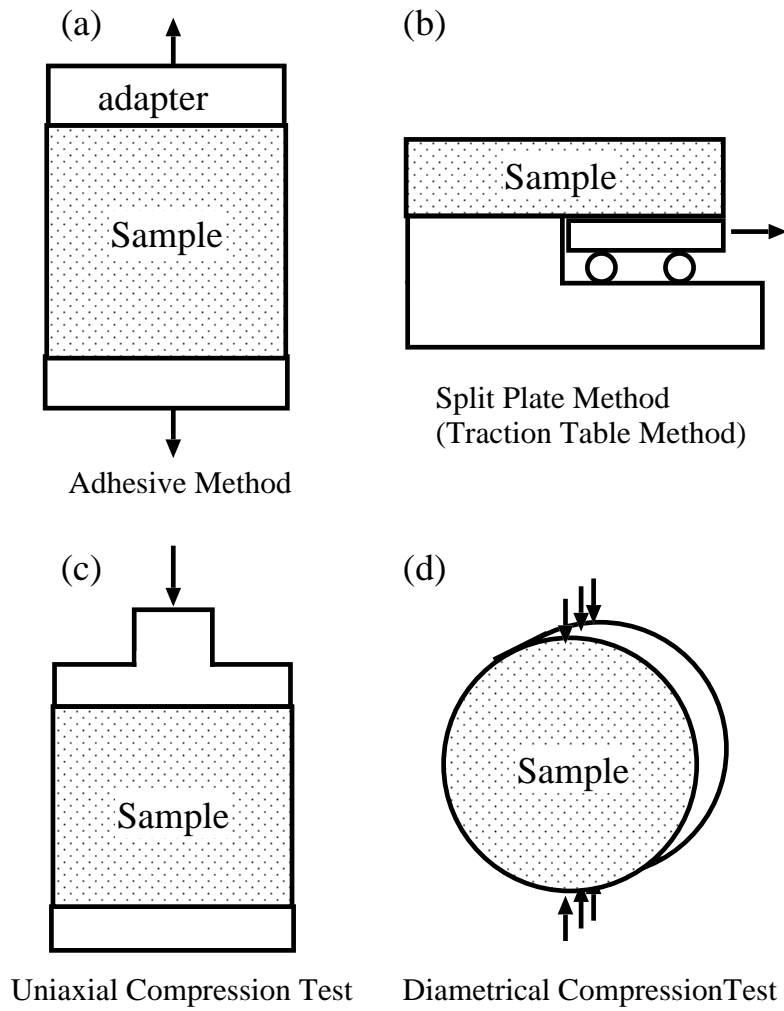


Figure 10. Several measurement techniques of strength of granular media. The adhesive method (a), the split-plate method (traction table method) (b), the uniaxial compression test (c), and the diametrical compression test (d).

**Test methods and Mohr circle.** Several experimental methods have been used to measure the tensile strength of wet granular media (e.g., [66, 67]). The simplest method is just to pull the sample apart until the material fails, as shown in Figs. 10(a) and (b). However, it is difficult to hold the sample because wet granular media are fragile and not always uniform. In the adhesive method (Fig. 10(a)), the material needs to be strong enough so that the bottom and top faces of the sample can be bonded to the adaptors. In the case of the split-plate method (Fig. 10(b)), the sample is placed on a plate, and the plate

is split until the material fails. In either method, both the stress and the strain can be measured until reaching failure.

The uniaxial and diametrical compression tests have also been conducted, where the sample is compressed in one direction until it fails. In uniaxial compression tests (Fig. 10(c)), a sample is pressed by a ram along one direction. In the case of the diametrical compression test, a linear load is applied to a sample of cylindrical shape across one diameter of the disk (Fig. 10(d)), and the tensile stress is calculated based on the Hertz theory for isotropic elastic bodies [68, 69], though the validity of the elastic theory for granular media with the assumption of the isotropy is rather suspicious.

In addition to these uniaxial tests, where only one component of the stress applied to the sample is controlled, there are methods where two components of the stress are separately controlled. The triaxial compression test has been widely performed for soils [28, 70, 71]. Figure 11(a) shows a schematic description of the triaxial testing system. The cylindrical-shaped sample is placed in a confining cell filled with fluid, and the sample is separated from the confining fluid by a flexible membrane. The sample is compressed from above by a ram, and the pressure at side membrane can be separately controlled by changing the pressure of the confining fluid. In the case of the direct shear test in Fig. 11(b), a sample in a shear box is sheared as the shear box is slid. A series of tests can be conducted by varying the vertical compressive stress from the top. Note that there are several modifications of these tests: In the case of unsaturated soils, the modified tests are often performed, where the suction is kept constant during the test by using the HAE material (see subsection 2.2.2) and allows the liquid to drain from the sample [28].

It should be noted that the sample needs to be prepared carefully in either method in order to get reproducible results. Especially, how the sample is compacted before the measurement is an important factor to determine its mechanical response.

The results of the tensile, compression, and shear tests are often analysed by using the Mohr circle, which visualises the rotational transformation of the two-dimensional stress tensor as follows [28, 70, 71]. Let us consider a two-dimensional stress tensor whose principal values are  $\sigma_1$  and  $\sigma_2$ . If the coordinate axes are rotated by an angle  $\alpha$  from the principal axes, the stress tensor  $\sigma_{ij}$  in the coordinate system is given by

$$\begin{aligned} \begin{pmatrix} \sigma_{11} & \sigma_{12} \\ \sigma_{21} & \sigma_{21} \end{pmatrix} &= \begin{pmatrix} \cos \alpha & \sin \alpha \\ -\sin \alpha & \cos \alpha \end{pmatrix} \begin{pmatrix} \sigma_1 & 0 \\ 0 & \sigma_2 \end{pmatrix} \begin{pmatrix} \cos \alpha & -\sin \alpha \\ \sin \alpha & \cos \alpha \end{pmatrix} \\ &= \begin{pmatrix} \frac{(\sigma_1 + \sigma_2)}{2} + \frac{(\sigma_1 - \sigma_2)}{2} \cos 2\alpha & \frac{(\sigma_1 - \sigma_2)}{2} \sin 2\alpha \\ \frac{(\sigma_1 - \sigma_2)}{2} \sin 2\alpha & \frac{(\sigma_1 + \sigma_2)}{2} - \frac{(\sigma_1 - \sigma_2)}{2} \cos 2\alpha \end{pmatrix} \quad (13) \end{aligned}$$

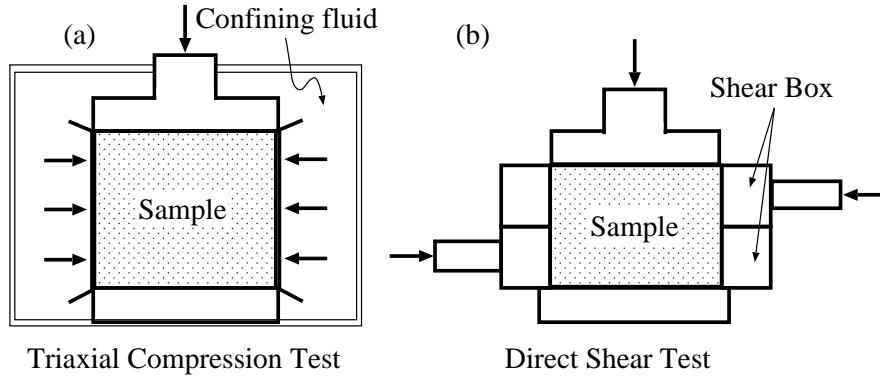


Figure 11. Schematic diagrams of a triaxial test system (a) and a direct shear test system (b).

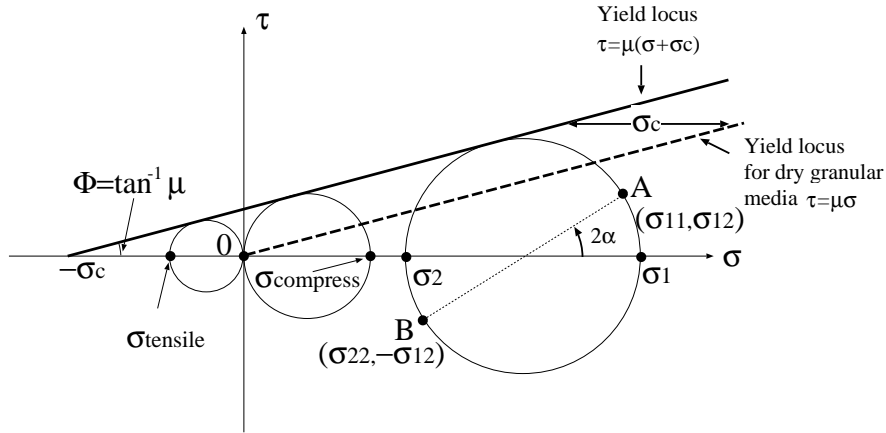


Figure 12. A schematic diagram of Mohr circles in the plane shear stress  $\tau$  versus normal compressive stress  $\sigma$ . When a two-dimensional stress tensor (whose  $(i, j)$  component is given by  $\sigma_{ij}$ ) is considered, the Mohr circle includes the diametrically-opposed points  $A(\sigma_{11}, \sigma_{12})$  and  $B(\sigma_{22}, -\sigma_{12})$ , as shown in the figure. The yield locus from the Mohr-Coulomb criterion for cohesive granular media is shown by the solid straight line, and the yield locus of the non-cohesive granular media is shown by the dashed line.

Namely, when we consider two points  $A(\sigma_{11}, \sigma_{12})$  and  $B(\sigma_{22}, -\sigma_{21})$  in the  $\tau - \sigma$  plane, they locate at the diametrically-opposed points on a circle

$$\left[ \sigma - \frac{1}{2}(\sigma_1 + \sigma_2) \right]^2 + \tau^2 = \left[ \frac{1}{2}(\sigma_1 - \sigma_2) \right]^2, \quad (14)$$

as shown in Fig. 12, where the angle between the  $\sigma$  axis and the line  $A - B$  is  $2\alpha$ .

The Mohr circle is useful when considering the Mohr-Coulomb criterion

Eq. (9). The stress at failure, from the Mohr-Coulomb criterion, gives a straight line

$$\tau = \mu(\sigma + \sigma_c) \quad (15)$$

in the  $\tau$ - $\sigma$  plane with  $\sigma$ -intercept at  $-\sigma_c$  and slope  $\mu$ . Instead of  $\mu$ ,  $\Phi = \tan^{-1} \mu$  (shown in Fig. 12) is also used as a parameter for the Mohr-Coulomb criterion;  $\Phi$  is called the internal friction angle. If the granular aggregate obeys the Mohr-Coulomb criterion, the Mohr circle at failure should be tangent to this straight line (15), because the granular aggregate fails as soon as a stress state that satisfies the criterion appears. Therefore, by drawing an envelope curve of Mohr circles at failure with various stress conditions, from the data one can construct the Mohr-Coulomb criterion to determine the parameters  $\mu$  and  $\sigma_c$ .

This procedure can be done for the triaxial compression test and the shear test, where two components of the stress tensor are varied separately. The granular material does not always follow the ideal Mohr-Coulomb criterion and the envelope might be curved, but the response is linear for small enough values of the stress, and this gives  $\mu$  and  $\sigma_c$ .

In the case of uniaxial tensile (compression) tests, one of the principal values is always zero. Thus, the resulting Mohr circle crosses the origin of the  $\sigma$ - $\tau$  plane, where the tensile (compressive) stress at failure is given by  $\sigma_{\text{tensile}}$  ( $\sigma_{\text{compress}}$ ) as shown in Fig. 12. For a given internal friction coefficient  $\mu$ ,  $\sigma_{\text{tensile}}$  ( $\sigma_{\text{compress}}$ ) is proportional to  $\sigma_c$ , and the behaviour of  $\sigma_{\text{tensile}}$  ( $\sigma_{\text{compress}}$ ) gives information about the cohesion in the wet granular medium. However, we cannot determine the cohesive stress  $\sigma_c$  from a uniaxial test unless we know  $\mu$  from another experiment.

Below let us briefly review some experimental results about the stresses at the failure state for wet granular media with various liquid content.

**Tests in the pendular state.** Pierrat *et al.* [72] investigated the Mohr-Coulomb criterion by using direct shear tests for various granular assemblies including monodisperse glass beads and polydisperse crushed limestone with relatively small liquid content. The amount of liquid was larger than that in the experiments on the angle of repose presented in subsection 3.1.2, but the system was supposed to be still in the pendular state.

The yield loci in shear test for glass beads of diameter  $93 \mu\text{m}$  with various liquid content are shown in Fig. 13, which shows a shift of the yield locus to the left from the dry case, but the slope is unchanged. It has also been found that the shift increases with the liquid content. For all the materials they investigated, they found that the yield loci can be collapsed by shifting the curve. Namely, in this experiment, the main effect of the liquid appears in the cohesive stress  $\sigma_c$ , but the internal friction coefficient  $\mu$  was not significantly



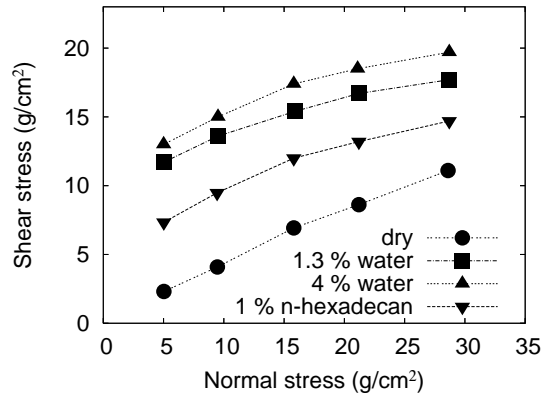


Figure 13. Yield locus obtained by direct shear tests for glass beads ( $93 \mu\text{m}$ ): Dry (circles), with water (1.3% of liquid content is shown by squares, and 4% of liquid content is shown by triangles), and with n-hexadecan (liquid content 1%, shown by upside-down triangles). Adapted from [72].

modified, which indicates that the effect of lubrication was small.

They also investigated the relation between the shear test and the uniaxial tensile test. They had conducted tensile tests separately [73], and from their empirical relation between  $\sigma_{\text{tensile}}$  and parameters that characterise the sample, such as packing fraction and liquid content, they estimated the tensile strength  $\sigma_{\text{tensile}}$  for the sample in the shear tests. If the internal friction coefficient  $\mu = \tan \Phi$  for dry samples does not change for wet granular materials, we can estimate  $\sigma_c$  from  $\sigma_{\text{tensile}}$ , using the relation  $\sigma_c = (1 + \sin \Phi)|\sigma_{\text{tensile}}|/(2 \sin \Phi)$  (see Fig. 12) with  $\Phi$  being the internal friction angle in the dry case. This estimation was compared with observed yield loci in shear tests, and reasonable agreement was found.

**Tests with intermediate liquid content.** Next, we review the tensile tests and uniaxial compression tests of wet granular media with intermediate liquid content, typically in the funicular state. The mechanical response of the funicular state is not well understood, because in this state even the qualitative dependence of the tensile strength (tensile stress at the peak of stress-strain relation) on liquid content varies from one material to another, and the reason for this is not very clear. Here we just summarise a few experiments.

In the field of agglomeration processing, experiments have been conducted from relatively dry to almost saturated conditions. However, in the funicular state, the liquid content dependence of the strength may either increase or decrease upon increasing the liquid content. For example, increasing tensile strength with increasing liquid content has been found by Schubert [74] for limestone with mean diameter  $65 \mu\text{m}$  using the adhesive method. Figure 14 shows the stress-strain relation for various liquid content  $S$ , and the peak stress

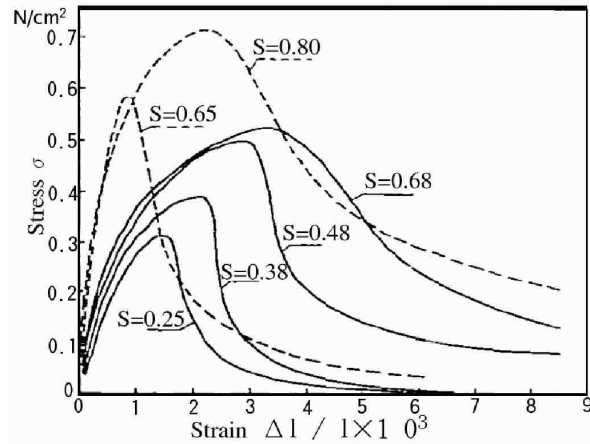


Figure 14. Stress-strain relation of wet limestone (mean diameter  $65 \mu\text{m}$ ) obtained by the adhesive method [74]. The packing fraction  $\nu$  of the sample was 0.66. The dashed lines show the result for a sample prepared by a drying process (drainage), while the solid lines show the result for a sample prepared by a wetting process (imbibition).  $S$  refers to the percentage liquid content. From [74].

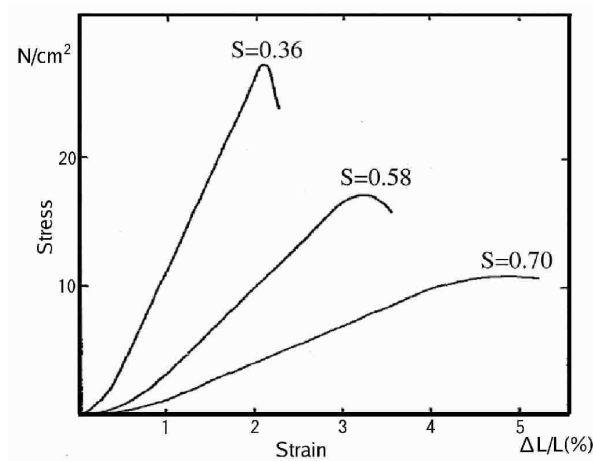


Figure 15. Stress-strain relation of dicalcium phosphate (diameter  $21 \mu\text{m}$ ) with an aqueous solution of a polymer.  $S$  refers to the percentage liquid content. The packing fraction of the sample was 0.5. From [75].

gives tensile strength. Stress-strain curves, showing decreasing strength as the liquid content  $S$  increases from 36% to 70% are shown in Fig. 15, from [75], where compressive tests were performed using dicalcium phosphate with diameter  $21 \mu\text{m}$ . Kristensen *et al.* [76] found increasing strength for increasing liquid content using glass beads of particle size  $68 \mu\text{m}$ , while decreasing strength for dicalcium phosphate of particle size  $14 \mu\text{m}$  in uniaxial compress-

sion tests. There have been many other experiments probing the mechanical strength of wet granular media (see [24] for a review). The effect of particle size on the competition between cohesion and lubrication was considered [24] to be one of the causes of these various behaviours, but the liquid content dependence in the intermediate liquid-content-regime (approximately given by  $20\% \lesssim S \lesssim 90\%$ ) is not yet well-understood.

It has been found that the critical strain  $\epsilon_c$  (strain at the peak in the stress-strain curve) always increases with increasing liquid content, as shown in Figs. 14 and 15. This indicates that the wet granular material is brittle when the amount of liquid is small, and tends to show visco-plastic behaviour as the liquid content is increased.

It should be also noted that, even for similar amounts of liquid content, the strength of a sample may depend on whether it is prepared by either draining or adding liquid; Schubert [74] found different stress-strain curves for each processes as shown in Fig. 14. In many studies, the sample is often driven by an external force (e.g., rotating drum, mixing, etc.) before the measurement in order to better distribute the liquid, which would make hysteresis less obvious.

**Tests in soil mechanics: relatively large amounts of liquid.** As pointed out in subsection 2.2.1, the suction in the capillary state largely varies upon a small change of liquid content. In soil mechanics, the shear tests of unsaturated soils have been conducted by decreasing the water content from initially saturated soils, or, in other words, by increasing the suction from zero. The data is usually presented in terms of the suction  $\Delta P$ , not the liquid content  $S$ . This is a reasonable way of arranging data in the capillary state, because the change of  $\Delta P$  upon changing  $S$  is very rapid for low and high liquid content as has been shown in subsection 2.2.1. Here we summarise these data to try to understand the mechanical properties with large amount of liquid content. It should be noted that the grains that form soils can be very small (for example, clay can be the order of  $2 \mu\text{m}$  in diameter), may have characteristic shape, and may be affected by, e.g., electrostatic interaction. These properties affect its mechanical responses, but we focus on the variation of the mechanical properties upon changing the suction  $\Delta P$  in the following, so that we will be able to extract the properties mainly determined by the capillary effect.

The failure condition given by the Mohr-Coulomb criterion in Eq. (9) has been experimentally investigated for soils. Figure 16(a) shows<sup>1</sup> the yield loci

---

<sup>1</sup>In soil mechanics, the total normal stress  $\sigma_t$ , the air pressure  $P_a$ , and the water pressure  $P_l$  are often taken to be the control parameters. Here, the total normal stress  $\sigma_t$  includes both the load on the granular sample and the fluid pressure on it, thus  $\sigma_t = P_a$  if the sample is placed in air without any external load. When an external pressure is applied on the sample, the net normal stress  $\sigma$  sustained by granular particles would be given by  $\sigma_t - P_a$ . In the original figures of Fig. 16(a), the label of the horizontal axis shows “Net Normal Stress  $\sigma - u_a$  (kPa)”, where  $\sigma$  in [28] represents the total normal stress, and  $u_a$  is the air pressure ( $\sigma_t$  and  $P_a$  in our notation, respectively).

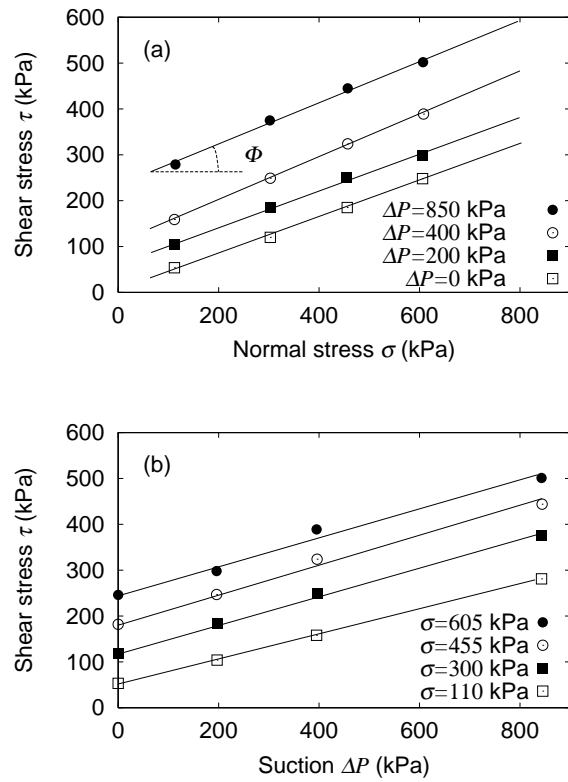


Figure 16. Yield loci for wet soil (Madrid Gray Clay). (a) Net normal stress  $\sigma$  versus shear stress  $\tau$  for various suction  $\Delta P = P_a - P_l$ . The slope is almost independent of suction in this regime. (b) Shear stress versus suction for various net normal stresses  $\sigma$ . The slope is almost independent of the net normal stress in this regime. Adapted from [28] (original data from [77]).

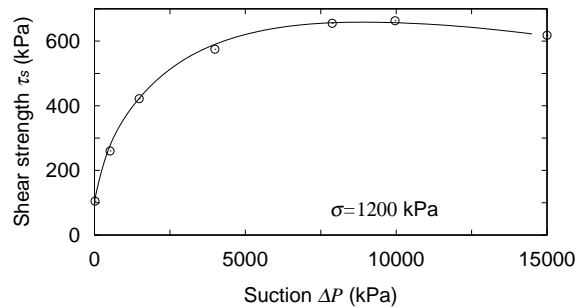


Figure 17. Shear strength  $\tau_s$  versus suction  $\Delta P$  obtained by shear tests for red clay. This figure shows a larger range of suction  $\Delta P$  (compared to Fig. 16(b)), as well as a non-linear and non-monotonic behaviour. Adapted from [78].

of wet clay for various values of the suction  $\Delta P$ , where the slope gives the friction coefficient  $\mu$  and the  $y$ -intercepts of lines give  $\mu\sigma_c$ . The slopes scarcely vary with suction, which indicates that  $\mu$ , or, the internal friction angle  $\Phi = \tan^{-1}\mu$ , does not depend on the suction  $\Delta P$ . The  $y$ -intercept is small for  $\Delta P = 0$  and increases with increasing the suction  $\Delta P$ . Namely,  $\sigma_c$  increases with increasing  $\Delta P$ .

Figure 16(b) shows the yield shear stress versus suction for various normal compressive stresses, which shows a linear dependence on  $\Delta P$ . This result and the fact that the internal friction angle  $\Phi$  depends little on the suction  $\Delta P$  suggest that the cohesive stress  $\sigma_c$  increases linearly with  $\Delta P$ . The linear increase of  $\sigma_c$  upon increasing  $\Delta P$  for small  $\Delta P$  is natural, because the compressive stress  $\Delta P$  at the liquid-air interface at the surface of the granular assembly is the source of the cohesion. This behaviour has been found for some kinds of clay [77–79], undisturbed decomposed granite [80], silt [81], and glacial till [82].

When  $\Delta P$  is increased further, a non-linear dependence of the shear strength  $\tau_s$  (the shear stress at failure for a given suction and normal load) on  $\Delta P$  is found [28, 78], as shown in Fig. 17. The increase of the shear strength  $\tau_s$  becomes nearly zero as  $\Delta P$  grows. It is very likely that the internal friction coefficient  $\mu$  does not vary significantly upon changing  $\Delta P$  in these regimes, and then the obtained shear strength  $\tau_s$  is proportional to the cohesive stress  $\sigma_c$ .

Summarising these results,  $\sigma_c$  increases linearly with  $\Delta P$  for small enough suction  $\Delta P$ , but for large  $\Delta P$ , the increase disappears. The suction  $\Delta P$  increases as the liquid content  $S$  decreases as shown in Fig. 5, therefore,  $\sigma_c$  increases upon decreasing the liquid content from  $S = 100\%$  ( $\Delta P = 0$ ) [83].

### 3.2 Dynamical behaviours

In this subsection, we briefly describe some dynamical behaviours of wet granular media. In the dynamical regime, not only cohesion but also other effects of the liquid such as viscosity, lubrication, and liquid motion play important roles. The dynamical behaviours observed are far more complicated than those in the quasistatic regime. In addition, though there are numerous studies of the dynamics of partially wet granular media from the practical point of view, systematic studies in simple situations are rather few; here we briefly summarise some of the experimental studies on the dynamical response of wet granular media. Those who are interested in recent studies on dynamics should also refer to a recent review [22].

#### 3.2.1 Dynamics in the pendular state.

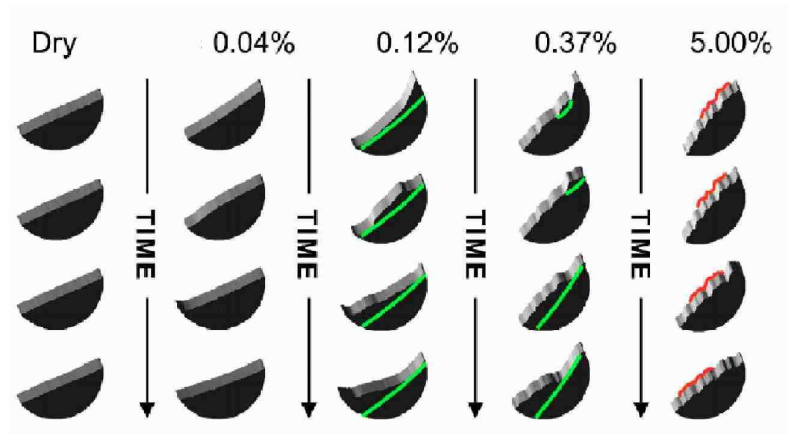


Figure 18. Surface shapes in a rotating drum during single avalanches, for various liquid contents  $S$  (shown as percentages). The coloured line for liquid content percentages 0.12% and 0.37% indicate approximate slip planes in the correlated regime, and the coloured lines for 5.00% show the travelling quasiperiodic surface features in the viscoplastic regime. From [84].

**Avalanches in rotating drums.** Granular flow and avalanches in a rotating drum have been widely investigated for dry granular media (see, e.g., [85–92]). At low rotation rate, the grains stay at rest until the surface angle reaches the critical angle  $\theta_c$ , and avalanche occurs; the angle just after the avalanche is the angle of repose  $\theta_r$ . This is called the intermittent regime. When the rotation rate is high enough, the continuous flow occurs with keeping a constant angle between the surface and horizontal plane; this is the continuous regime. The flow regimes of fine cohesive powders in a rotating drum has been also studied by [93].

Tegzes *et al.* [84, 94] investigated the flow behaviours of wet granular materials in a thin rotating drum. In the experiments, the amount of liquid is small (liquid content varied from 0.001% to 5%), where the pendular state is expected. They have observed the transition from intermittent to continuous flow with increasing the rotation rate in this range of liquid content.

They observed the time evolution of the surface profile, which enable them to calculate the mean surface angle, statistics of the local surface angle, evolution of pattern at the surface, etc. In Fig. 18, the typical surface profiles just after avalanches in the intermittent flow regime are shown. For enhanced clarity, the gray-scale plot in the third dimension of the figure shows the local surface angles.

By changing the liquid content, the following three regimes have been distinguished. For low liquid content, the cohesion is small, and small avalanches are observed (the *granular* regime); the avalanches occur at the surface and the surface profile is always smooth (Fig. 18, liquid content 0.04%), similarly

to the dry granular media (Fig. 18, dry case). When increasing the liquid content, the cohesion becomes stronger, and grains move as a connected block. An avalanche occurs through a succession of local slip events, and the surface structure fluctuates after each avalanche; this is the *correlated* regime (Fig. 18, liquid content 0.12% and 0.37%). Further increasing the liquid content results in the *visco-plastic* regime. In this state, the flow becomes coherent over the entire sample, and fluctuations are suppressed (Fig. 18, liquid content 5%).

They also found that the critical angle  $\theta_c$  depends not only on the liquid content but also on the rotation rate. They varied the duration between avalanches, or the “waiting time”, from about 0.1 s to 1000 s. It was found that  $\theta_c$  increased logarithmically with the waiting time. They supposed that this was caused by the slow flow of liquid along the particle surface.

A systematic study of liquid motion in wet granular media in the pendular state was recently conducted by [62]. They found that, just after shaking the material to mix the liquid with grains, the average liquid bridge volume was much less than that in equilibrium; the volume saturated after long enough waiting times, more than one hour. This also suggests that the liquid-moving process is very slow and may induce the ageing effect observed by [84, 94].

***Vibrated wet granular media.*** Dry granular media placed on a horizontal plane excited by vertical vibrations is a fundamental and widely-used setup to study granular gases (e.g., [95]), segregation (e.g., [96]), and pattern formation (e.g., [97]). In dry granular media, the onset of fluidisation is often characterised by the dimensionless acceleration  $\Gamma = A\omega^2/g$ , where  $A$  is the amplitude of the vibration,  $\omega$  is the angular frequency of the vibration, and  $g$  is the acceleration of gravity. There is a threshold  $\Gamma_{\min}$  below which there are no fluidisation, which was reported to be a constant around one, (e.g., [1, 98, 99]), but recently reported that  $\Gamma_{\min}$  can be smaller than one and show weak  $\omega$  dependence [100, 101]. Above the fluidisation threshold, dry granular media exhibits transitions between localised patterns of jumping grains (in the case of few layers of grains) all the way to gas-like phases (see, e.g., [102–108]).

For wet granular media, the cohesion force introduces an additional force or energy scale. It is non-trivial to determine which parameters would better characterise the resulting behaviour. Recently, experiments on this subject have been conducted [27, 109], where fluidisation of glass beads wet by water under vertical vibration has been investigated. The critical dimensionless acceleration  $\Gamma_{\text{crit}}$  for fluidisation is found to depend on the frequency  $f = \omega/2\pi$ , the particle radius  $R$ , and the liquid content  $W$  defined as the ratio of the liquid volume to the total volume, as shown in Fig. 19. Here,  $W$  is defined as the ratio of the liquid volume to the total volume. They [27, 109] found that  $\Gamma_{\text{crit}}$  depends weakly on  $f$ , but becomes constant for sufficiently high frequency. In this high frequency regime [27, 109],  $\Gamma_{\text{crit}}$  is smaller for larger  $R$  for a given  $W$

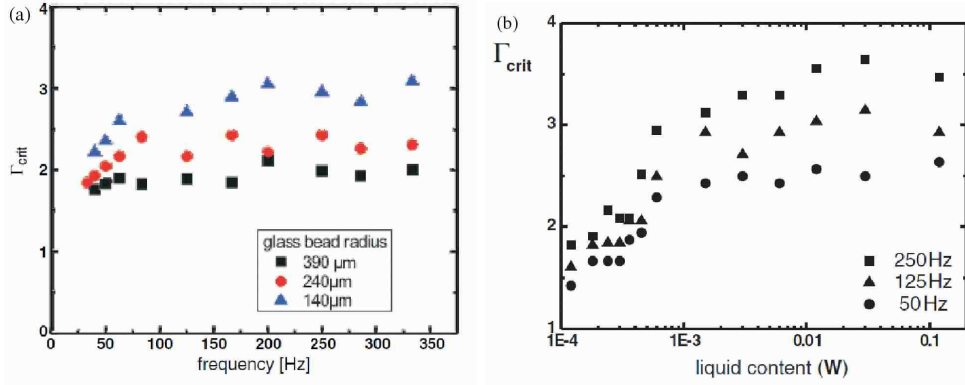


Figure 19. (a) Critical acceleration  $\Gamma_{crit}$  versus frequency  $f$  for three different bead radii, with water content  $W = 0.5\%$ . (b)  $\Gamma_{crit}$  versus liquid content  $W$  for three different frequencies. The particle radius  $R$  is  $140 \mu\text{m}$ . From [27].

(Fig. 19(a)), while it increases with  $W$  for a given  $R$  (Fig. 19(b)).

Ref. [27,109] interpreted their results by considering the cohesion force due to liquid bridges between grains as well as between grains and the container wall. The increase of  $\Gamma_{crit}$  with  $W$  was found [109] to be proportional to the increase of the cohesion force  $F_{bridge}$  per liquid bridge, which they estimated from  $W$ . It is natural that  $\Gamma_{crit}$  increases with increasing  $F_{bridge}$ , but [27,109] found that the proportionality is not trivial: Another possibility is that  $\Gamma_{crit}$  is ruled by the energy required to break the bridge, whose dependence on  $W$  should be different from the dependence of the force. In the case of the dependence upon  $R$ , [27,109] explained it by considering the shear stress due to the formation of liquid bridges between grains and side walls; the bulk material tends to move together due to the cohesion, but if the shear from the side wall is large enough, the shear stress makes it possible to deform the bulk sample and to induce the fluidisation. Following their interpretation, the decrease of  $\Gamma_{crit}$  upon increasing  $R$  is because the force per bridge is proportional to  $R$  but the number of liquid bridges per area is proportional to  $1/R^2$ , which gives the shear stress proportional to  $1/R$ . They [27,109] also studied the fluidisation with the container whose walls are covered by the hydrophobic material so that liquid bridges cannot be formed with the side walls, and they found that the material cannot be fluidised up to  $\Gamma = 20$ .

**Segregation.** Segregation of grains by their size is one of the most striking phenomena of granular materials. The most well-known example is the Brazil-nuts effect, i.e., the large Brazil-nuts always appear on top of mixed-nuts containers. After two or more kinds of grains are mixed together, size segregation occurs very easily when they are excited by an external energy input



in, e.g., a vibrated container or chute flows. Size-segregation has been studied for dry granular material for various types of mixtures and excitations (e.g., [96,110–112]). In wet granular materials, the cohesion tends to suppress the segregation by sticking grains together, but at the same time, various factors come into play in such a dynamical situation, as we will see below.

The size-segregation in wet granular materials that flow down an inclined plane has been investigated in [113,114]. They used binary mixtures of glass beads with several sets of diameters. Also water, glycerol, and other kinds of liquid were used to observe the effect of the viscosity as well as the surface tension. They found that segregation is basically suppressed by increasing the liquid content, which is natural because the cohesion tends to suppress the particles' relative motion.

Samadani and Kudrolli [113,114] investigated the phase diagrams of segregation in the space of particle diameter ratio and liquid content. These found a qualitative difference of phase diagrams between water and glycerol: the surface tensions are almost the same for these two kinds of liquid, but the viscosities are different, and the segregation is lower at higher viscosity. This is because [113,114] viscosity tends to reduce the velocity fluctuations required for segregation.

Samadani and Kudrolli [113,114] estimated the viscous force between moving particles connected by a liquid bridge by using the Reynolds lubrication theory, in which the hydrodynamic effect in thin space is taken into account [15,16,115,116]. There [113,114], the force is proportional to the relative velocity between moving particles, and they found that the viscous force can be comparable with the cohesive force for the characteristic velocity scale under gravity. This also suggests that the viscosity is very important for dynamical behaviour like segregation.

On the other hand, Geromichalos *et al.* [22,117] investigated size segregation in granular media in a jar driven by a horizontal circular motion (Fig. 20(a)). They found that segregation sometimes occurs partially, and they investigated the degree of segregation by measuring the fraction of the mixture zone (i.e., the region where no segregation occurs) to the total sample. From the experiments, they distinguished three regimes: (Fig. 20(b)); the *gaseous* regime, where an increase of the liquid content enhances size-segregation; the *intermediate* regime, where segregation occurs, but increasing the liquid content suppresses segregation; and the *viscoplastic* regime, where no segregation occurs. By increasing the liquid content with a fixed ratio of radii, the system state evolves from gaseous, intermediate, to the viscoplastic regimes.

The behaviour in the gaseous regime found in [117], where segregation is enhanced by increasing liquid content, seems to contradict the results in [113,114]. Geromichalos *et al.* [117] discussed that, in the gaseous regime, the energy dissipation is enhanced by the breakage of a number of tiny liquid

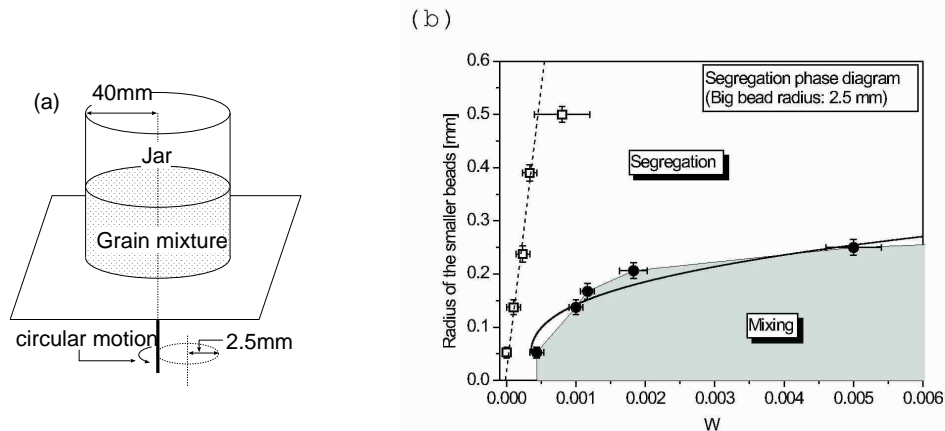


Figure 20. (a) Schematic description of the experimental setup in [22,117]. The jar experience rapid, horizontal circular motions (20 revolutions per second), where the centre of the jar follows a small circle as shown in the figure (The jar itself is not spinning around its centre). (b) Particle-size segregation phase diagram for binary mixtures of wet granular materials. The radius of the bigger beads is fixed, and the vertical axis shows the radius of the smaller beads. The horizontal axis shows the amount of liquid via the dimensionless quantity  $W$ , defined as the volume of the liquid divided by the total volume of the small beads (including the space between the beads). The segregation does not occur in grey region. The dashed steep line separates the region where the segregation is enhanced by adding water (left) from the region where the segregation decreases or stays the same (right). From [117].

bridges, while the cohesion is not enough to strongly affect the dynamics. The larger energy dissipation tends to enlarge the energy difference between large and small grains, resulting in an enhanced segregation. As liquid content is increased, the liquid bridge becomes larger and the kinetic energy becomes insufficient to break the bridges [117]. Then, segregation is suppressed and the system goes from the intermittent regime to the viscoplastic regime.

**3.2.2 Shear experiments for various liquid content.** Recently, Fournier *et al.* [27] investigated the response of wet granular materials under shear by using a unique experimental setup, shown in Fig. 21. A cylindrical cell was filled with spherical glass beads wet by water, where the flat sides of the cell (area  $A$ ) each consist of a thin latex membrane. Adjacent to each membrane was a cylindrical chamber filled with liquid, connected to a syringe. When the pistons of the syringe are moved at equal speed, the membranes are deformed by a volume  $\Delta V$  (Fig. 21(a) shows a lateral cut of the cylindrical cell (top) and a vertical cut (bottom)), which allows them to shear the granular material under a constant volume at a controlled speed. The pressure at each membrane is measured during the shear. The pressure difference  $\Delta\sigma$  between the two membranes versus average shear  $\Delta V/A$  is shown in Fig. 21(b) for densely packed glass

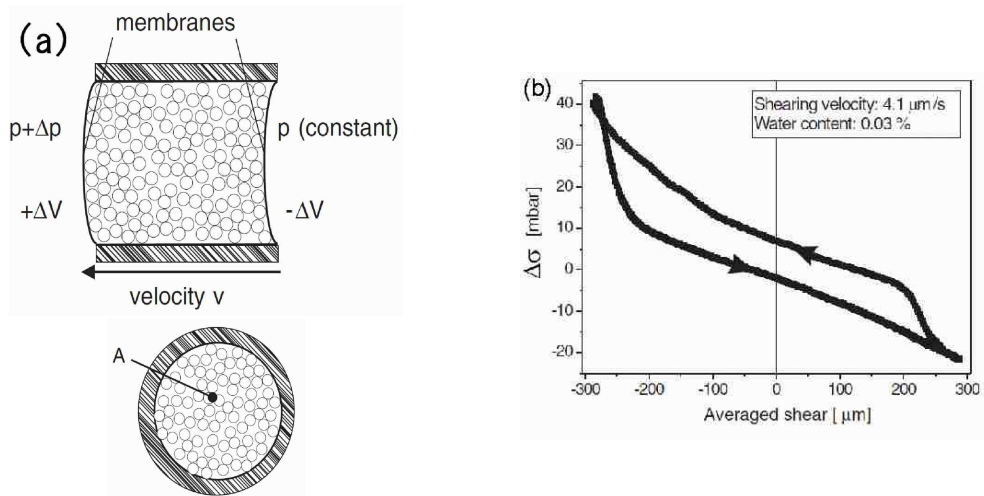


Figure 21. (a) Experimental setup to shear wet granular materials in a cell, showing a slice of the shearing cell seen from the side and from the front. (b) The hysteresis loop of the pressure difference  $\Delta\sigma$  versus the average shear  $\Delta V/A$  for densely packed glass beads. From [27].

beads (packing fraction  $\nu \approx 0.63$ ), showing hysteresis. The vertical width of the hysteresis loop reflects the resistance to shear of the material. They defined  $\Delta\sigma_0$  as the vertical width of the hysteresis loop at zero strain divided by two, and measured  $\Delta\sigma_0$  for various liquid content and shear rate. The dependence of  $\Delta\sigma_0$  upon the amount of wetting liquid is shown in Fig. 22. Following their parametrisation, the horizontal axis shows  $W$ , the ratio of the liquid volume to the total volume. For a given packing fraction  $\nu$ , the liquid saturation  $S$  is given by  $S = W/(1 - \nu)$ , thus  $W = 0.35$  is almost in a saturated state ( $S \approx 0.95$ ) when  $\nu = 0.63$ . We can see that  $\Delta\sigma_0$  increases rapidly as  $W$  is increased from zero, but it starts to drop at  $W \approx 0.04$  ( $S \approx 0.1$ ) and goes to zero at  $W \approx 0.35$ . They observed the liquid distribution for small liquid content by index matching techniques, and found that  $W \approx 0.03$  is the point where liquid bridges start to merge to form a liquid cluster (Fig. 23); beyond that point, the interfaces between the air and liquid start to decrease, which may cause the decrease of the cohesive force.

Reference [27] also investigated the shear rate dependence of  $\Delta\sigma_0$ . Within the investigated range of the shear rate,  $\Delta\sigma_0$  decreases for larger shear rate, while the dry granular material does not show shear-rate dependence. A possible origin of the shear-rate dependence is the time dependence of liquid motion as described in section 3.2.1, which affect the temporal evolution of liquid bridges.

In addition, they [27] claim that the increase of the shear stress is not solely coming from the frictional effect, as in the Mohr-Coulomb picture described in section 3.1.2, but it can be understood by just considering the cohesion that

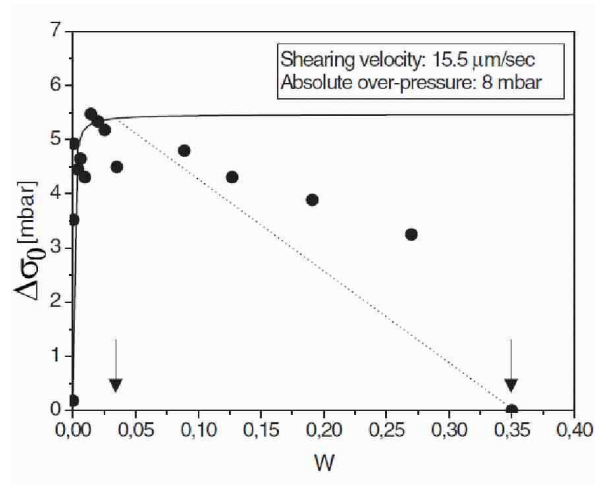


Figure 22. Dependence of  $\Delta\sigma_0$  upon the amount of the liquid  $W$ . From [27].

arises from the liquid bridges. One of the tests they conducted to confirm their claim is to measure the absolute pressure dependence of  $\Delta\sigma_0$ ; if the frictional shear stress proportional to the cohesive normal stress  $\sigma_c$  is responsible for the fact that  $\Delta\sigma_0$  is greater than that of the dry granular material, then applying a unidirectional pressure comparable with  $\sigma_c$  for *dry* granular material may cause a similar effect to increase  $\Delta\sigma_0$ . However, they found that applying absolute pressure to the sample is not enough to make  $\Delta\sigma_0$  increase. Though the fact that the applied pressure is unidirectional while the cohesive pressure is uniform may be one of the causes of this difference [22], their results indicates that the origin of the higher yield shear stress in wet granular materials need to be investigated further.

The response of materials against shear is a fundamental property to understand the material's rheology. Further experiments of sheared wet granular material in various setups would be useful.

**3.2.3 Dynamics of wet granular media: practical applications.** There are many research fields that investigate the dynamics of wet granular media from a practical point of view. Below we summarise a few examples.

**Agglomeration processing: grains binded by liquid.** During an agglomeration or granulation process, particles lump or agglomerate together into larger, semi-permanent aggregates called granules [24, 118, 131]. There are several methods to make granules. One of them is to spray a binder liquid onto dry powder and mix them in, e.g., a tumbling drum so that clumps of particles

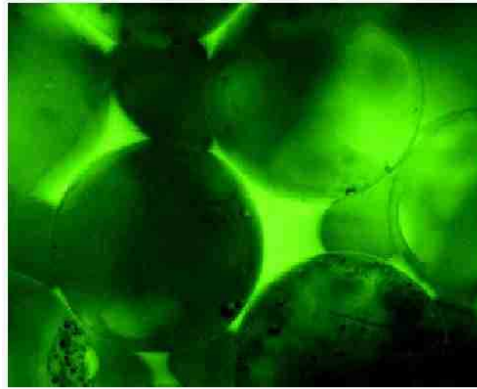


Figure 23. Fluorescence microscope images of liquid distribution between glass beads of diameter  $375\ \mu\text{m}$  for  $W = 0.03$ , “liquid clusters” are formed. From [27].

binded by liquid grows. The granules may either grow or break down when they collide. Another method is to strongly shear a very dense mixture of binder liquid and powder (dense paste), and then air comes into the paste to form lumps. In either method, the main source of the cohesive force that binds powder particles together is the capillary force.

Numerous dynamical experiments have been performed on granulation processing: The dynamics of liquid distribution during granulation, the growth of granules, the shear rate dependence of the growth rate, the collision velocity dependence of breakage, and so on. Though most of the experimental setups seem rather complicated, the accumulated knowledge provides many insights on the dynamical properties of wet granular media. However, it is beyond the scope of this brief review to summarise all experiments in this subfield. Interested readers should consult a rather recent review on this topic [24], a conference proceedings [118], and references therein.

In addition, the properties of sheared dense paste are important not only in the granulation process, but also in, e.g., ceramics engineering, where the rheology of paste has been investigated. The importance of cohesion due to the capillary effect in the rheology of paste has often been pointed out (e.g., [119, 120]), and the knowledge about its rheology also provides insights about wet granular media.

**Geological events.** Geology is one of the largest research fields on wet granular media. The failure criterion of soils and also their dynamical behaviours are very important to understand. Significant, and sometimes catastrophic and tragic, examples include land slides, debris flows, and liquefaction of ground (see, e.g., [71, 121–124]).

Most of the past work on debris flows focused on the flow of soils saturated by

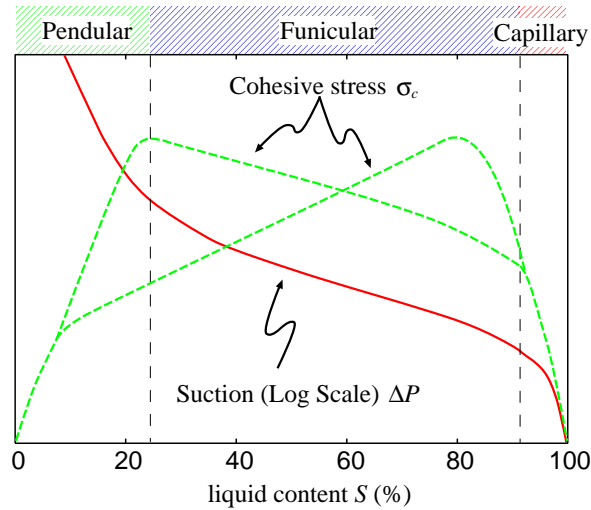


Figure 24. Schematic diagram summarising the variations of the suction  $\Delta P$  and the cohesive stress  $\sigma_c$ , upon changing the liquid content  $S$ .

water. In studies of debris flows, knowledge about dry granular media has been incorporated into the analysis, and at the same time, the significant effects of the liquid lubrication and the liquid viscosity on debris flows have been investigated [121]. Liquefaction of wet soils triggered by earthquakes is also often studied in saturated situations [71]. Systematic studies of wet granular media from partially-wet to the completely wet state should also provide useful insights to understand these important geological events.

## 4 Summary and open questions

### 4.1 Effect of the liquid content on quasistatic behaviour

The cohesive force due to the presence of a liquid arises in the pendular, funicular, and capillary states. This cohesion gives rise to a finite cohesive stress in quasistatic experiments. Figure 24 shows a schematic diagram summarising how the suction  $\Delta P$  and the cohesive stress  $\sigma_c$  vary upon liquid content.

The dependence of the suction  $\Delta P$  on the liquid content  $S$  is given by a red solid line, and its slope changes significantly near the phase boundaries between the pendular, funicular, and capillary states, as discussed in subsection 2.2.1.

The cohesive stress  $\sigma_c$  versus  $S$  is schematically shown by the green dashed lines. The overlapping dashed curves for low and high  $S$  are better established, while the non-overlapping intermediate curves vary significantly between experiments. The cohesive stress  $\sigma_c$  increases as we add more and more liquid

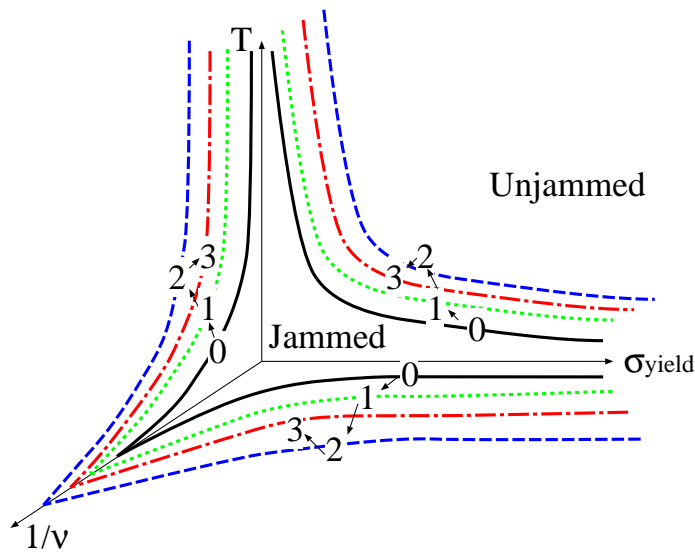


Figure 25. Schematic diagram of a possible jamming phase diagram of granular media for various liquid contents. Number 0 (black solid line): Dry . Number 1 (green dotted line): Small amount of liquid (slightly cohesive). Number 2 (blue dashed line): “Optimal” amount of liquid (the most cohesive, and the largest phase-space volume of the jammed phase). Number 3 (red dash-dotted line): Large amount of liquid (less cohesive than the optimal case).

to initially dry grains, shown by the positive slope, for small  $S$ , of the  $\sigma_c$  line in the pendular state. At the opposite end, cohesion becomes zero for completely saturated granular media ( $S = 100\%$ ), schematically shown by the green dashed line with negative slope for  $S$  close to 100% in the capillary state.

In the funicular state, the cohesive stress  $\sigma_c$  dependence on the liquid content  $S$  is not clearly understood. The cohesive stress  $\sigma_c$  may either increase or decrease with  $S$  in the funicular state. These possible curves are shown by the green dashed lines, where both lines connect to single lines in the limits when  $S \rightarrow 0$  and  $S \rightarrow 100\%$ . We see that there would be at least one maximum of the cohesive stress at a certain liquid content, though it is not clear, a priori, the location of the peak.

#### 4.2 Open problems

There are a number of open problems on mechanical properties of wet granular media, some of which have already been mentioned in the text. In this subsection, we list a few examples of open problems, in order to encourage future studies in this area.

**4.2.1 Jamming.** As summarised in subsection 4.1, in the quasistatic regime, the cohesion in wet granular media has a maximum for a certain liquid content, though whether the maximum is located at a rather small or large liquid content is not known a priori. This variable cohesion will affect the “jamming” properties of the granular assembly. Thus, an interesting problem worth considering is the jamming phase diagram in wet granular media.

A jammed state occurs when a disordered system subject to an external force is caught in a small region of phase space with no possibility of escape [104, 108, 125–130]. In order to unjam a jammed material, a finite yield stress or fluctuation energy is needed, which forces the elements to escape from the phase space region where they are trapped. Granular media at rest is a typical jammed material, where we need a finite yield stress or external energy input in order to let the grains flow or move. There are many kinds of materials that show jamming, such as dense colloids, and pinned vortices in superconductors. Jamming also plays a role in the mechanical properties of wet granular media. For example, Cates *et al.* [131] recently tried to understand the physics of granulation (section 3.2.3) in a highly-sheared dense paste in terms of a jamming transition under shear.

Liu *et al.* [125] proposed a very schematic phase diagram for jamming, in the space of packing fraction  $\nu$  (density), external load, and temperature or fluctuation energy. The purpose of this schematic phase diagram is to try to summarise a unified view of the jamming phenomena, observed in various media. A schematic diagram of our jamming phase diagram is shown in Fig. 25; the solid black curves, labelled with the number 0, was proposed by [127, 128] for non-cohesive (dry) granular media. The axes shown are: inverse packing fraction  $1/\nu$ , the yield stress  $\sigma_{\text{yield}}$ , and the fluctuating energy  $T$  from an external energy source, such as vibration. One of the features of jamming in dry granular media is that the behaviour in the  $T = 0$  plane, i.e., no external energy, can be easily investigated. The “jammed” phase-boundary intersects the inverse packing fraction  $1/\nu$  axis at zero yield stress and temperature, and the packing fraction at the intersection corresponds to the random closed-packing density [127, 128].

Obviously, attractive interactions modify the jamming properties. Trappe *et al.* [129] investigated jamming in colloidal systems with varying attractive interaction potentials; they found that the jammed phase boundary shifts to higher temperatures for stronger attractive potentials, because the attractive potential characterises the energy that particles need to escape from the phase space where they are trapped. Jamming in cohesive powders was investigated by [130]; the powder particles were large enough so that thermal noise was negligible. It was found that the critical jamming density for zero fluctuation energy and yield stress for cohesive powder is smaller than the critical density in non-cohesive granular media. This is because the cohesion made it possible



to form very sparse but stable clusters of powder. Indeed, a percolating cluster appears in their system for relatively low densities.

Considering these results, the cohesion present in wet granular media will decrease the density needed to jam the system. To break a cluster in wet granular media, a large enough external fluctuation energy is needed, and this energy will increase with cohesion. The yield stress will increase with cohesion as described by the Mohr-Coulomb criterion, where the yield shear stress increases with the cohesive stress  $\sigma_c$ . These considerations imply that, for cohesive granular media, the volume of phase space occupied by the jammed state expands as the cohesion increases.

How is the jammed phase diagram for granular media modified by adding liquid? A schematic phase diagram is shown in Fig. 25. The number in each curve there shows how the behaviour changes as we increase liquid content. When a small amount of liquid is added, the phase boundaries are slightly shifted so that the jammed phase expands in all three directions of  $1/\nu$ ,  $\tau$ , and  $T$  (number 1, green dotted lines). As liquid is further added, the cohesion *increases*, and the boundary will shift further. At a certain liquid content, the cohesion will reach a maximum, corresponding to the *largest jammed region* in phase space (number 2, blue dashed lines). As we further increase the liquid content, the cohesion *decreases*, and the phase-space volume of the jammed region decreases (number 3, red dash-dotted line). Namely, as far as cohesion is concerned, there is an optimal liquid content that maximises the jammed region. This argument does not consider the effects of liquid other than cohesion. For large enough liquid content, the lubrication effect may affect this conclusion, and could drastically shrink the size of the jammed region. The liquid content dependence of the jamming behaviour in wet granular media is an important and interesting phenomenon that has not been systematically investigated and constitutes a fertile new direction of research.

**4.2.2 Statistical mechanics approach.** Recently, many physicists are trying to describe dry granular systems using statistical mechanics approaches, especially in the jammed regime (For a recent review, see [132]).

Edwards [12, 133] postulated that a dense granular assembly under small external perturbations can take all possible jammed configurations, and the density can be described by suitable ensemble averages over its blocked states. Later, Nowak *et al.* [41] investigated the compaction of slowly tapped granular assemblies, and found there exists a “reversible regime”: When a loosely packed configuration is tapped, large voids are removed, which results in irreversible motion of grains (the initial loosely packed configuration cannot be reproduced by further tapping). Once the memory of this initial configuration is lost, after large enough tapping, the density is determined by the ratio  $\Gamma$  of the tapping

amplitude to gravity, which is in the reversible regime; in this regime, the density is lower for larger  $\Gamma$ . The existence of a reversible regime is non-trivial in granular matter, where the frictional force depends on history. The Edwards’ scenario only considers non-history dependent situations, and the existence of such a regime gives hope that this scenario would work in the reversible regime. Research to test this theory has been done [134–140], and there remains many open questions.

Another example of a statistical mechanics approach is the recent experiment by [104], who observed the motion of a torsion oscillator immersed in a granular medium perturbed by external vertical tapping, and measured the susceptibility and the auto-correlation function of the motion of the oscillator. For the equilibrium systems, these two quantities are related by the fluctuation-dissipation theorem and the temperature can be consistently determined. They [104] examined whether the same formalism works in the granular state, and found that an “effective temperature” can be defined from the susceptibility and the auto-correlation function. Though this dissipative system is far from equilibrium, the analogy to the fluctuation-dissipation theorem in the experiment is remarkable. It is an interesting question whether such a relation can be extended to other systems or regimes (e.g., wet grains).

In the case of wet granular media, the available phase space is larger and, due to the cohesion, the history dependence is stronger than the dry case as mentioned in Section 3.1.1 and Table 1. Future experiments probing the statistical mechanics in wet granular assemblies will provide more knowledge of its applicability and generality.

**4.2.3 *Arches and contact-force fluctuations.*** Arches (i.e., effective long-range interactions) and the resulting large fluctuation of contact forces have been extensively studied in several types of dry granular media (see, e.g., [141–147]). However, no such systematic studies exist for wet granular media. The clogging of cohesive powders in a hopper is often said to be an arching effect [3], but it is rather rare to investigate the arches directly in partially wet granular media. This would be interesting because the change of the inter-particle forces with liquid content likely affects the strength and topology of the so-called “force chains” or stress-line-networks of the granular assembly.

**4.2.4 *Simple experimental setups to study the dynamics of wet granular media.*** Several experimental setups have been widely performed to study the fundamental dynamics of dry granular media. The widely-used setups include vibrated granular media (e.g., [96, 102–108]), rotating drums (e.g., [85–92]), shear (e.g., [145, 148–150]), and inclined chutes (e.g., [13, 151–159]). These

setups have played important roles in studying the fundamental dynamics and rheology of dry granular materials.

Some of the setups have been used in recent experiments of wet granular media, as discussed in section 3.2, but not so many systematic studies have been done so far. One of the difficulties in fundamental studies of wet granular materials is their strong tendency to be inhomogeneous. It becomes difficult to induce particle motions, due to cohesive force. In other words, the regions that were mobile in the dry case become localised when wet, and the bulk material becomes solid. Similar behaviours are known for dry granular materials as well (e.g., shear bands), but the localisation would be stronger for the wet case. In addition, the distribution of liquid can also be inhomogeneous, especially for larger liquid content. Nonetheless, further studies on the dynamics of wet granular materials (including their inhomogeneity) using these rather simple setups will certainly contribute to granular science.

**4.2.5 Numerical simulations.** The recent remarkable progress in the study of dry granular material is partially due to numerical simulations. Molecular dynamics simulations of soft-sphere or inelastic hard-sphere models help clarify phenomena found in experiments and get data in “ideal” situations. In the case of wet granular media, however, its numerical simulation model for the wide range of liquid content has not been established yet because of its complexity.

Some models of wet grains in the pendular state have been proposed for molecular dynamics simulations (e.g., [24, 51, 118, 160–163]), where most of them are based on soft-particle models for dry granular materials with elastic force and dissipation [164]. In models for wet grains, the effect of the liquid is added by assuming that liquid bridges are formed when grains are in contact, and cohesion and dissipation due to the liquid bridges are taken into account. These types of models would be applicable to some extent to situations where the amount of liquid is small and the liquid mostly sticks to the grain surface. However, as the liquid content is increased, the liquid-bridge picture becomes invalid and liquid motion becomes relevant. No available simple models has been yet proposed for this regime, as far as we know.

Even for dry granular media, the real granular particles are more complicated than the ones used in most computational models; still, the simple models have been found to be very useful. It is apparent that good models are also needed for wet granular material. The required level of realism of the model largely depends on the phenomena that one would like to understand. To help the modelling, more systematic experiments in simple situations are necessary.

**4.2.6 Mechanical properties of snow.** The mechanical properties of snow have been investigated for a long time (e.g., [54, 165–169]). It is important to understand snow properties to reduce disasters caused by snow avalanches; thus knowledge should also be useful to design equipment and constructions in snowbound areas [169].

Snow is a type of granular material of grains of ice. Snow partially melts in many situations, and pores are filled with both air and water; it is a “wet granular material”. The knowledge obtained about the dynamics of dry granular media has been found to be useful to understand snow dynamics; for example, the mechanism of size segregation is important to understand how to save skiers caught in an avalanche [167]. In terms of cohesion among grains, wet snow avalanches has some aspects in common with avalanches in partially wet granular media [84]. More research on wet granular media should be useful to better understand the mechanical properties of snow.

However, there is a big difference between wet sands and snow; in snow, solid ice-bonds exist between ice grains. In new or low-density snows, ice grains slide over each other, while in old or dense snow, the deformation of solid ice-bonds dominate the interactions [167]. The formation, strength, and breakage of ice-bonds depend on many factors such as the heat flux and motion of water or water vapours. Because of this complex nature of interactions, there remains many open questions in snow physics. For example, it is known that the density of snow is not a good parameter to characterise snow properties, and one needs to classify snow by considering its microstructure [169]. It will be useful to find a parameter that is easily measured and can better characterise its mechanical properties.

## 5 Conclusion

Wet granular media have properties which are significantly different from dry grains. These include enhanced cohesion among grains leading to very steep angles of repose. Wet granular media are pervasive everywhere, including numerous industrial applications and geological phenomena. In spite of the ubiquitous presence of wet granular media and its importance, relatively little is known about it. This brief overview sketched some of the physical properties of wet granular media, and identified several open problems for future studies.

## Acknowledgements

NM thanks H. Nakanishi for helpful discussions. Authors thank G. D’Anna for his comments on an early version of the manuscript. Part of this work has

been done when NM was supported by the Special Postdoctoral Researcher Program by RIKEN. NM is supported in part by a Grant-in-Aid for Young Scientists(B) 17740262 from The Ministry of Education, Culture, Sports, Science and Technology (MEXT) and Grant-in-Aid for Scientific Research (C) 16540344 from Japan Society for the Promotion of Science (JSPS). FN is supported in part by the National Security Agency (NSA) and Advanced Research and Development Activity (ARDA) under Air Force Office of Research (AFOSR) contract number F49620-02-1-0334, and by the National Science Foundation grant No. EIA-0130383.

## References

- [1] J. Duran, *Sands, Powders, and Grains: An Introduction to the Physics of Granular Materials* (Springer, New York, 1997).
- [2] H.M. Jaeger, S.R. Nagel, and R.P. Behringer, *Granular solids, liquids, and gases*, Rev. Mod. Phys. **68** 1259 (1996).
- [3] R.M. Nedderman, *Statics and Kinematics of Granular Matter* (Cambridge University Press, Cambridge, 1992).
- [4] P.-G. de Gennes, *Granular matter: a tentative view*, Rev. Mod. Phys. **71** S374 (1999).
- [5] R.P. Behringer and J.T. Jenkins, editors *Powders & Grains 97*. (A. A. Balkema, Rotterdam, 1997).
- [6] R.A. Bagnold, *The Physics of Blown Sand and Desert Dunes*, (Mathuen, London, 1941).
- [7] H.M. Jaeger and S.R. Nagel, *Physics of the granular state*, Science **255** 1523 (1992).
- [8] H.M. Jaeger, S.R. Nagel, and R.P. Behringer, *The physics of granular materials*, Physics Today **49** 32 (1996).
- [9] P. Sholtz, M. Bretz, and F. Nori, *Sound-producing sand avalanches*, Contemporary Physics **38** 329 (1997).
- [10] F. Nori, P. Sholtz, and M. Bretz, *Booming sand*, Scientific American **277** 84 (1997).
- [11] R.P. Behringer, H.M. Jaeger, and S.R. Nagel, editors. *Focus issue on granular materials*, Chaos, **9** 509 (1999).
- [12] S.F. Edwards and D.V. Grinev. *Granular materials: towards the statistical mechanics of jammed configurations*, Adv. Phys. **51** 1669 (2002).
- [13] M. Bretz, J.B. Cunningham, P.L. Kurczynski, and F. Nori, *Imaging of avalanches in granular materials*, Phys. Rev. Lett. **69** 2431 (1992).
- [14] Kansai International Airport Co. Ltd. *Brief summary of settlement*, <http://www.kiac.co.jp/english/land/land.htm>.
- [15] Y. Kimura and H. Okabe. *Tribology Gairon (in Japanese)*, (Yokendo, Tokyo, 1994).
- [16] O. Pinkus and B. Sternlicht. *Theory of Hydrodynamic Lubrication*, (McGraw-Hill, New York, 1961).
- [17] F.P. Bowden and D. Tabor. *The Friction and Lubrication of Solids* (Clarendon Press, Oxford, 1986).
- [18] J.-C. Géminard, W. Losert, and J.P. Gollub. *Frictional mechanics of wet granular material*, Phys. Rev. E **59** 5881 (1999).
- [19] M. Medved, H.M. Jaeger, and S.R. Nagel. *Convection in a fully immersed granular slurry*, Phys. Rev. E **63** 061302 (2001).
- [20] L.D. Landau and E.M. Lifshitz. *Fluid Mechanics* (Butterworth-Heinemann, Oxford, 2nd edition, 1987).
- [21] C.D. Willett, M.J. Adams, S.A. Johnson, and J.P.K. Seville, *Capillary bridges between two spherical bodies*, Langmuir **16** 9396 (2000).
- [22] S. Herminghaus, *Dynamics of wet granular matter*, Adv. Phys. **54** 221 (2005).
- [23] D.M. Newitt and J.M. Conway-Jones, *A contribution to the theory and practice of granulation*, Trans. I. Chem. Eng. **36** 422 (1958).
- [24] S.M. Iveson, J.D. Litster, K. Hapgood, and B. J. Ennis, *Nucleation, growth and breakage phenomena in agitated wet granulation processes: a review*, Powder Technol. **117** 3 (2001).
- [25] M.A. Rubio, C.A. Edwards, A. Dougherty, and J.P. Gollub, *Self-affine fractal interfaces from*

- immiscible displacement in porous media*, Phys. Rev. Lett. **63** 1685 (1989).
- [26] T.G. Mason, A.J. Levine, D. Ertas, and T.C. Halsey, *Critical angle of wet sandpiles*, Phys. Rev. E **60** R5044 (1999).
- [27] Z. Fournier, D. Geromichalos, S. Heminghaus, M.M. Kohonen, F. Mugele, M. Scheel, M. Schulz, B. Schulz, Ch. Schier, R. Seemann, and A. Skudelný, *Mechanical properties of wet granular material*, J. Phys.: Condens. Matter **17** S477 (2005).
- [28] N. Lu and W.J. Likos. *Unsaturated Soil Mechanics*. (John Wiley & Sons, Hoboken, 2004).
- [29] D.K. Cassel and A. Klute, *Water potential: tensiometry*, in A. Klute, editor, *Methods of Soil Analysis, Part 1, Physical and Mineralogical Methods, 2nd ed.* (Soil Science Society of America, Madison, WI, 1986).
- [30] D.I. Stannard, *Tensiometers—theory, construction, and use*, Geotech. Test. J. **15** 48 (1992).
- [31] J.W. Hilf. *An investigation of pore water pressure in compacted cohesive soils* (Technical report, United States Department of the Interior, Bureau of Reclamation, Design and Construction Division, Denver, CO, 1956).
- [32] K.A. Bocking and D.G. Fredlund. *Limitations of the axis translation technique*, In *Proceedings of the 4th International Conference on Expansive Soils*, pp. 117–135 (Denver, CO, 1980).
- [33] C.J. Phene, G.J. Hoffman, and S.L. Lawlings, *Measuring soil matric potential in-situ by sensing heat dissipation within a porous body: I. theory and sensor construction*, Soil Science Society of America Proceedings **35** 27, (1971).
- [34] C.J. Phene, G.J. Hoffman, and S.L. Lawlings. *Measuring soil matric potential in-situ by sensing heat dissipation within a porous body: II. experimental results*, Soil Science Society of America Proceedings **35** 225 (1971).
- [35] D.G. Fredlund and D.K.H. Wong. *Calibration of thermal conductivity sensors for measuring soil suction* Geotech. Test. J. **12** 188 (1989).
- [36] S.L. Houston, W.N. Houston, and A. Wagner. *Laboratory filter paper suction measurements* Geotech. Test. J. **17** 185 (1994).
- [37] P.-G. de Gennes. *Wetting: statics and dynamics* Rev. Mod. Phys. **57** 827 (1985).
- [38] P.-G. de Gennes, D. Quere, and F. Brochard-Wyart, *Capillarity and Wetting Phenomena: Drops, Bubbles, Pearls, Waves* (Springer-Verlag, Berlin, 2003).
- [39] M. Alava, M. Dubé, and M. Rost, *Imbibition in disordered media*, Adv. Phys. **53** 83 (2004).
- [40] J.B. Knight, C.G. Fandrich, C.N. Lau, H.M. Jaeger, and S.R. Nagel, *Density relaxation in a vibrated granular material*, Phys. Rev. E **51** 3957 (1995).
- [41] E.R. Nowak, J.B. Knight, E. Ben-Naim, H.M. Jaeger, and S.R. Nagel, *Density fluctuations in vibrated granular materials*, Phys. Rev. E **57** 1971 (1998).
- [42] M. Nicodemi, A. Coniglio, and H.J. Herrmann, *Frustration and slow dynamics of granular packings*, Phys. Rev. E **55** 3962 (1997).
- [43] J.Q. Xu, R.P. Zou, and A.B. Yu, *Packing structure of cohesive spheres* Phys. Rev. E **69** 032301 (2004).
- [44] G. Gioia, A.M. Cuitiño, S. Zheng, and T. Uribe, *Two-phase densification of cohesive granular aggregates*, Phys. Rev. Lett. **88** 204302 (2002).
- [45] C.M. Kong and J.J. Lannutti, *Localized densification during the compaction of alumina granules: The stage I–II transition*, J. Am. Ceram. Soc. **83** 685 (2000).
- [46] L. Bocquet, E. Charlaix, S. Ciliberto, and J. Crassous, *Moisture-induced ageing in granular media and the kinetics of capillary condensation*, Nature **396** 735 (1998).
- [47] D.J. Hornbaker, R. Albert, I. Albert, A.-L. Barabási, and P. Schiffer, *What keeps sandcastles standing* Nature **387** 765 (1997).
- [48] R. Albert, I. Albert, D. Hornbaker, P. Schiffer, and A.-L. Barabási, *Maximum angle of stability in wet and dry spherical granular media*, Phys. Rev. E **56** R6271 (1997).
- [49] N. Fraysse, H. Thomé, and L. Petit, *Humidity effects on the stability of a sandpile*, Euro. Phys. J. B **11** 615 (1999).
- [50] T.C. Halsey and A.J. Levine, *How sandcastles fall*, Phys. Rev. Lett. **80** 3141 (1998).
- [51] S.T. Nase, W.L. Vargas, A.A. Abatan, and J.J. McCarthy, *Discrete characterization tools for cohesive granular material*, Powder Technol. **116** 214 (2001).
- [52] F. Restagno, C. Ursini, H. Gayvallet, and E. Charlaix, *Aging in humid granular media*, Phys. Rev. E **66** 021304 (2002).
- [53] G. Ovarlez, E. Kolb, and E. Clement, *Rheology of a confined granular material*, Phys. Rev. E **64** 060302 (2001).
- [54] G. D’Anna, *Mechanical properties of granular media, including snow, investigated by a low-frequency forced torsion pendulum*, Phys. Rev. E **62** 982 (2000).
- [55] G. D’Anna, *Dissipative dynamics of granular media investigated by forced torsion pendulum*,

- Europhys. Lett. **51** 293 (2000).
- [56] A.J. Forsyth, S. Hutton, and M.J. Rhodes, *Effect of cohesive interparticle force on the flow characteristics of granular material* Powder Technol. **126** 150 (2004).
- [57] J. Crassous, L. Bocquet, S. Ciliberto, and C. Laroche, *Humidity effect on static aging of dry friction*, Europhys. Lett. **47** 562 (1999).
- [58] J.N. Israelachvili, *Intermolecular and Surface Forces* (Academic Press, New York, 2nd edition, 1992).
- [59] N. Olivi-Tran, N. Fraysse, P. Girard, M. Ramonda, and D. Chatain, *Modeling and simulations of the behavior of glass particles in a rotating drum in heptane and water vapor atmospheres* Eur. Phys. J. B **25** 217 (2002).
- [60] H. Rumpf, *The strength of granules and agglomerates*, In William A. Knepper, editor, *Agglomeration*, pp.379 (Interscience publishers, New York, 1962).
- [61] J.W. Cahn and R.B. Heady, *Analysis of capillary forces in liquid-phase sintering of jagged particles*, J. Am. Ceram. Soc. **53** 406 (1970).
- [62] M.M. Kohonen, D. Geromichalos, M. Scheel, C. Schier, and S. Herminghaus, *On capillary bridges in wet granular materials*, Physica A **339** 7 (2004).
- [63] P. Tegzes, R. Albert, M. Paskvan, A.-L. Barabási, T. Vicsek, and P. Schiffer, *Liquid-induced transitions in granular media*, Phys. Rev. E **60** 5823 (1999).
- [64] D. Ertas, T.C. Halsey, A.J. Levine, and T.G. Mason, *Stability of monomer-dimer piles*, Phys. Rev. E **66** 051307 (2002).
- [65] S. Nowak, A. Samadani, and A. Kudrolli, *Maximum angle of stability of a wet granular pile*, Nature Physics **1** 50 (2005).
- [66] D.G. Bika, M. Gentzler, and J.N. Michaels, *Mechanical properties of agglomerates*, Powder Technol. **117** 98 (2001).
- [67] H. Schubert, *Tensile strength of agglomerates*, Powder Technol. **11** 107 (1975).
- [68] A.T. Procopio, A. Zavaliangos, J.C. Cunningham, *Analysis of the diametrical compression test and the applicability to plastically deforming materials*, J. Materials Sci. **38** 3629 (2003).
- [69] H. Hertz, *Gesammelte Werke (Collected Works)* (Leipzig, 1895).
- [70] Á. Kézdi, *Soil Physics (Handbook of Soil Mechanics, Vol. 1)* (Elsevier, Amsterdam, 1974).
- [71] F. Oka, *Soil Mechanics (Doshitsu-Rikigaku, in Japanese)* (Asakura-Shoten, Tokyo, 2003).
- [72] P. Pierrat, D.K. Agrawal, and H.S. Caram, *Effect of moisture on yield locus of granular materials: theory of shift*, Powder Technol. **99** 220 (1998).
- [73] P. Pierrat and H.S. Caram, *Tensile strength of wet granular materials*, Powder Technol. **91** 83 (1997).
- [74] H. Schubert, W. Herrmann, and H. Rumpf, *Deformation behaviour of agglomerates under tensile stress*, Powder Technol. **11** 121 (1975).
- [75] H.G. Kristensen P. Holm, T. Schaefer, *Granulation in high-speed mixers: Part V. power consumption and temperature changes during granulation*, Powder Technol. **43** 213 (1985).
- [76] H.C. Kristensen, E. Holii, and T. Schaefer, *Mechanical properties of moist agglomerates in relation to granulation mechanisms: Part I. deformability of moist, densified agglomerates*, Powder Technol. **44** 227 (1985).
- [77] V. Escario, *Suction-controlled penetration and shear tests* In *Proceedings of the 4th International Conference on Expansive Soils*, pp. 781–787 (Denver, CO, 1980).
- [78] V. Escario, J. Juca, and M.S. Coppe, *Strength and deformation of partly saturated soils* In *Proceedings of the 12th International Conference on Soil Mechanics and Foundation Engineering*, **3** pp. 43–46 (Rio de Janeiro, 1989).
- [79] A.W. Bishop, I. Alpan, G.E. Blight, and I.B. Donald, *Factors controlling the shear strength of partly saturated cohesive soils*, In *ASCE Research Conference on the Shear Strength of Cohesive Soils*, pp. 503–532 (University of Colorado, Boulder, 1960).
- [80] D.Y.F. Ho and D.G. Fredlund, *increase in shear strength due to suction for two Hong Kong soils*, In *Proceedings of the ASCE Geotechnical Conference Engineering and Construction in Tropical and Residual Soils* (Honolulu, HI, 1982).
- [81] J. Krahn, D.G. Fredlund, and M.J. Klassen, *Effect of soil suction on slope stability at notch hill*, Can. Geotech. J. **26** 269 (1989).
- [82] J.K.M. Gan, D.G. Fredlund, and H. Rahardjo, *Determination of shear strength parameters of an unsaturated soil using the direct shear test*, Can. Geotech. J. **25** 500 (1988).
- [83] S.K. Vanapalli, D.G. Fredlund, D.E. Pufahl, and A.W. Clifton, *Model for the prediction of shear strength with respect to soil suction*, Can. Geotech. J. **33** 379 (1996).
- [84] P. Tegzes, T. Vicsek, and P. Schiffer, *Development of correlations in the dynamics of wet granular avalanches*, Phys. Rev. E **67** 051303 (2003).

- [85] J. Rajchenbach, *Flow in powders: From discrete avalanches to continuous regime*, Phys. Rev. Lett. **65** 2221 (1990).
- [86] J. Rajchenbach, *Dynamics of grain avalanches*, Phys. Rev. Lett. **88** 014301 (2002).
- [87] D. Bonamy, F. Daviaud, L. Laurent M. Bonetti, and J.P. Bouchaud, *Multiscale clustering in granular surface flows*, Phys. Rev. Lett. **89** 034301 (2002).
- [88] J. Rajchenbach, *Granular flows*, Adv. Phys. **49** 229 (2000).
- [89] V.G. Benza, F. Nori, and O. Pla, *Mean-field theory of sandpile avalanches: From the intermittent- to the continuous-flow regime*, Phys. Rev. E **48** 4095 (1993).
- [90] G.H. Ristow, *Dynamics of granular materials in a rotating drum*, Europhys. Lett. **34** 263 (1996).
- [91] D.V. Khakhar, J.J. McCarthy, T. Shinbrot, and J.M. Ottino, *Transverse flow and mixing of granular materials in a rotating cylinder*, Phys. Fluids **9** 31 (1997).
- [92] G. Baumann, J.M. Janosi, and D.E. Wolf, *Surface-properties and flow of granular material in a 2-dimensional rotating-drum model*, Phys. Rev. E **51** 1879 (1995).
- [93] A. Castellanos, J.M. Valverde, A.T. Perez, A. Ramos, and P.K. Watson, *Flow regimes in fine cohesive powders*, Phys. Rev. Lett. **82** 1156 (1999).
- [94] P. Tegzes, T. Vicsek, and P. Schiffer, *Avalanche dynamics in wet granular materials*, Phys. Rev. Lett. **89** 094301 (2002).
- [95] T. Poschel and S. Luding, editors, *Granular Gases*, volume 564 of *Lecture Notes in Physics*. (Springer-Verlag, Berlin, 2001).
- [96] A. Kudrolli, *Size separation in vibrated granular matter*, Rep. Prog. Phys. **67** 209 (2004).
- [97] G.H. Ristow, *Pattern Formation in Granular Materials* (Springer-Verlag, Berlin, 2000).
- [98] E. Clément, J. Duran, and J. Rajchenbach, *Experimental study of heaping in a two-dimensional "sandpile"* Phys. Rev. Lett. **69** 1189 (1992).
- [99] J. B. Knight, H. M. Jaeger, and S. R. Nagel, *Vibration-induced size separation in granular media: The convection connection*, Phys. Rev. Lett. **70** 3782 (1993).
- [100] S. Renard, T. Schwager, T. Pöschel, and C. Salueña, *Vertically shaken column of spheres. onset of fluidization*, Eur. Phys. J. E **4** 233 (2001).
- [101] T. Pöschel, T. Schwager, and C. Salueña, *Onset of fluidization in vertically shaken granular material*, Phys. Rev. E **62** 1361 (2000).
- [102] W. Losert, D.G.W. Cooper, and J.P. Gollub, *Propagating front in an excited granular layer*, Phys. Rev. E **59** 5855 (1999).
- [103] F. Melo, P.B. Umbanhowar, and H.L. Swinney, *Hexagons, kinks, and disorder in oscillated granular layers*, Phys. Rev. Lett. **75** 3838 (1995).
- [104] G. D'Anna, P. Mayor, A. Barrat, V. Loreto, and F. Nori, *Observing Brownian motion in vibration-fluidized granular media*, Nature **424** 909 (2003).
- [105] P.B. Umbanhowar, F. Melo, and H.L. Swinney, *Localized excitations in a vertically vibrated granular layer*, Nature **382** 793 (1996).
- [106] H.K. Pak and R.P. Behringer, *Bubbling in vertically vibrated granular-materials*, Nature **371** 231 (1994).
- [107] C. Laroche, S. Douady, and S. Fauve, *Convective flow of granular masses under vertical vibrations*, J. Physique **50** 699 (1989).
- [108] G. D'Anna and G. Gremaud, *Vibration-induced jamming transition in granular media*, Phys. Rev. E **64** 011306 (2001).
- [109] M. Schell, D. Geromichalos, and S. Herminghaus, *Wet granular matter under vertical agitation*, J. Phys.: Condens. Matter **16** S4213 (2004).
- [110] M.E. Mobius, B.E. Lauderdale, S.R. Nagel, and H.M. Jaeger, *Brazil-nut effect - size separation of granular particles*, Nature **414** 270 (2001).
- [111] D.C. Hong, P.V. Quinn, and S. Luding, *Reverse Brazil nut problem: Competition between percolation and condensation*, Phys. Rev. Lett. **86** 3423 (2001).
- [112] J.M. Ottino and D.V. Khakhar, *Mixing and segregation of granular materials*, Annu. Rev. Fluid Mech. **32** 55 (2000).
- [113] A. Samadani and A. Kudrolli, *Segregation transitions in wet granular matter*, Phys. Rev. Lett. **85** 5102 (2000).
- [114] A. Samadani and A. Kudrolli, *Angle of repose and segregation in cohesive granular matter*, Phys. Rev. E **64** 051301 (2001).
- [115] O. Pitois, P. Moucheront, and X. Chateau, *Liquid bridge between two moving spheres: An experimental study of viscosity effects* J. Colloid Interface Sci. **231** 26 (2000).
- [116] O. Pitois, P. Moucheront, and X. Chateau, *Rupture energy of a pendular liquid bridge*, Euro. phys. J. B **23** 79 (2001).
- [117] D. Geromichalos, M.M. Kohonen, F. Mugele, and S. Herminghaus, *Mixing and condensation*



- in a wet granular medium*, Phys. Rev. Lett. **90** 168702 (2003).
- [118] A.D. Salman and M.J. Hounslow, editors. *Special Issue: 1st Int. Workshop on Granulation, Powder Technol.* **140** pp.155–296 (2004).
- [119] J.S. Reed, *Principles of Ceramics Processing* (John Wiley & Sons, New York, 2nd edition, 1995).
- [120] H. Van Damme, S. Mansoutre, P. Colombet, C. Lesaffre, and D. Picart, *Pastes: lubricated and cohesive granular media*, C. R. Physique **3** 229 (2002).
- [121] R.M. Iverson, *The physics of debris flows*, Rev. Geophys. **35** 245 (1997).
- [122] R. Dikau, D. Brunnsden, L. Schrott, and M.-L. Ibsen, *Landslide Recognition* (Wiley, Chichester, 1996).
- [123] P. Coussot, *Mudflow Rheology and Dynamics* (Balkema, Rotterdam, 1997).
- [124] K. Ishihara, *Liquefaction and flow failure during earthquakes*, Geotechnique **43** 351 (1993).
- [125] A.J. Liu and S.R. Nagel, *Jamming is not just cool any more*, Nature **396** 21 (1998).
- [126] A.J. Liu and S.R. Nagel, editors, *Jamming and Rheology: Constrained Dynamics on Microscopic and Macroscopic Scales* (Taylor & Francis, London, 2001).
- [127] C.S. O’Hern, S.A. Langer, A.J. Liu, and S.R. Nagel, *Random packings of frictionless particles*, Phys. Rev. Lett. **88** 075507 (2002).
- [128] C.S. O’Hern, L.E. Silbert, A.J. Liu, and S.R. Nagel, *Jamming at zero temperature and zero applied stress: The epitome of disorder* Phys. Rev. E **68** 011306 (2003).
- [129] V. Trappe, V. Prasad, L. Cipelletti, P.N. Segre, and D.A. Weitz, *Jamming phase diagram for attractive particles*, Nature **411** 772 (2001).
- [130] J.M. Valverde, M.A.S. Quintanilla, and A. Castellanos, *Jamming threshold of dry fine powders*, Phys. Rev. Lett. **92** 258303 (2004).
- [131] M.E. Cates, M.D. Haw, and C.B. Holmes, *Dilatancy, jamming, and the physics of granulation*, J. Phys.: Condens. Matter **17** S2517 (2004).
- [132] P. Richard, M. Nicodemi, R. Delannay, P. Ribi re, and D. Bideau, *Slow relaxation and compaction of granular systems*, Nature Materials **4** 121 (2005).
- [133] S.F. Edwards, *The role of entropy in the specification of a powder*, in *Granular Matter: An Interdisciplinary Approach*, pp. 121–140 (Springer, New York, 1994).
- [134] J.J. Brey, A. Padros, and B. Sanchez-Rey, *Thermodynamics description in a simple model for granular compaction*, Physica A **275** 310 (2000).
- [135] G. Tarjus and P. Viot, *Statistical mechanical description of the parking lot model for vibrated granular materials*, Phys. Rev. E **69** 011307 (2004).
- [136] M. Nicodemi, *Dynamical response functions in models of vibrated granular media*, Phys. Rev. E **82** 3734 (1999).
- [137] A. Coniglio and M. Nicodemi, *A statistical mechanics approach to the inherent states of granular media*, Physica A **296** 451 (2001).
- [138] H.A. Makse and J. Kurchan, *Testing the thermodynamic approach to granular matter with a numerical model of a decisive experiment*, Nature **415** 614 (2002).
- [139] A. Fierro, M. Nicodemi, and A. Coniglio, *Thermodynamics and statistical mechanics of frozen systems in inherent states*, Phys. Rev. E **66** 061301 (2002).
- [140] M. Nicodemi, A. Fierro, and A. Coniglio, *Segregation in hard spheres mixtures under gravity. an extension of edwards approach with two thermodynamics parameters*, Europhys. Lett. **60** 684 (2002).
- [141] R.R. Hartley and R.P. Behringer, *Logarithmic rate dependence of force networks in sheared granular materials*, Nature **421** 928 (2003).
- [142] I. Albert, P. Tegzes, B. Kahng, R. Albert, J.G. Sample, M. Pfeifer, A.-L. Barab si, T. Vicsek, and P. Schiffer, *Jamming and fluctuations in granular drag*, Phys. Rev. Lett. **84** 5122 (2000).
- [143] C.-h. Liu, S.R. Nagel, D.A. Schecter, S.N. Coppersmith, S. Majumdar, O. Narayan, and T.A. Witten, *Force fluctuations in bead packs*, Science **269** 513 (1995).
- [144] D. Howell, R.P. Behringer, and C. Veje, *Stress fluctuations in a 2d granular Couette experiment: A continuous transition*, Phys. Rev. Lett. **82** 5241 (1999).
- [145] B. Miller, C. O’Hern, and R.P. Behringer, *Stress fluctuations for continuously sheared granular materials*, Phys. Rev. Lett. **77** 3110 (1996).
- [146] S.N. Coppersmith, C.-h. Liu, S. Majumdar, O. Narayan, and T. A. Witten, *Model for force fluctuations in bead packs*, Phys. Rev. E **53** 4673 (1996).
- [147] D.L. Blair, N.W. Mueggenburg, A.H. Marshall, H.M. Jaeger, and S.R. Nagel, *Force distributions in three-dimensional granular assemblies: Effects of packing order and interparticle friction*, Phys. Rev. E **63** 041304 (2001).
- [148] H. Xu, M.Y. Louge, and A. Reeves, *Solutions of the kinetic theory for bounded collisional*

- granular flows*, Continuum Mech. Thermodyn. **15** 321 (2003).
- [149] D.M. Mueth, G.F. Debregeas, G.S. Karczmar, P.J. Eng, S.R. Nagel, and H.M. Jaeger, *Signatures of granular microstructure in dense shear flows*, Nature **406** 385 (2000).
- [150] S. Nasuno, A. Kudrolli, and J.P. Gollub, *Friction in granular layers: Hysteresis and precursors*, Phys. Rev. Lett. **79** 949 (1997).
- [151] T. Pöschel, *Granular material flowing down an inclined chute - a molecular-dynamics simulation*, J. Physique II **3** 27 (1993).
- [152] N. Mitarai, H. Hayakawa, and H. Nakanishi, *Collisional granular flow as a micropolar fluid*, Phys. Rev. Lett. **88** 174301 (2002).
- [153] N. Mitarai and H. Nakanishi, *Hard-sphere limit of soft-sphere model for granular materials: Stiffness dependence of steady granular flow*, Phys. Rev. E **67** 021301 (2003).
- [154] N. Mitarai and H. Nakanishi, *Linear stability analysis of rapid granular flow down a slope and density wave formation*, J. Fluid Mech. **507** 309 (2004).
- [155] N. Mitarai and H. Nakanishi, *Bagnold scaling, density plateau, and kinetic theory analysis of dense granular flow*, Phys. Rev. Lett. **94** 128001 (2005).
- [156] O. Pouliquen, *Scaling laws in granular flows down rough inclined planes*, Phys. Fluids **11** 542 (1999).
- [157] A. Daerr and S. Douady, *Two types of avalanche behaviour in granular media*, Nature **399** 241 (1999).
- [158] S.B. Savage and K. Hutter, *The motion of a finite mass of granular material down a rough incline*, J. Fluid Mech. **199** 177 (1989).
- [159] T.S. Komatsu, S. Inagaki, N. Nakagawa, and S. Nasuno, *Creep motion in a granular pile exhibiting steady surface flow*, Phys. Rev. Lett. **86** 1757 (2001).
- [160] T. Gröger, U. Tüzün, and D.M. Heyes, *Modelling and measuring of cohesion in wet granular materials*, Powder Technol. **133** 203 (2003).
- [161] M. Schulz, B.M. Schulz, and S. Herminghaus, *Shear-induced solid-fluid transition in a wet granular medium*, Phys. Rev. E **67** 052301 (2003).
- [162] G. Lian, C. Thornton, and M.J. Adams, *Discrete particle simulation of agglomerate impact coalescence*, Chem. Eng. Sci. **58** 3381 (1998).
- [163] M. Hakuno and K. Meguro, *Simulation of concrete-frame collapse due to dynamic loading*, J. Eng. Mech.-ASCE **119** 1709 (1993).
- [164] P.A. Cundall and O.D.L. Strack, *Discrete numerical model for granular assemblies*, Geotechnique **29** 47 (1979).
- [165] M. Fukue, *Mechanical performance of snow under loading* (Tokai University Press, Tokyo, 1979).
- [166] F. Nicor, *Constitutive modelling of snow as a cohesive-granular material*, Gran. Matt. **6** 47 (2004).
- [167] P. Bartelt and B. Othmar, *Avalanche physics ploughs ahead*, Physics World **14** 25 (2001).
- [168] G. Seligman *Snow structure and ski fields* (MacMillan and co., London, 1936).
- [169] L.H. Shapiro, J.B. Johnson, M. Sturm, and G.L. Blaisdell, *Snow mechanics: Review of the state of knowledge and applications* (Cold Regions Research and Engineering Laboratory Report, No. 97-3, 1997).